2017

Parametric study of helmholtz resonator performance and effect of poroacoustic material use in resonator design

Yasaman Esandiari
Iowa State University

Parametric study of Helmholtz resonator performance and effect of poroacoustic material use in resonator design

by

Yasaman Esfandiari

A thesis submitted to the graduate faculty

in partial fulfillment of the requirements for the degree of

MASTER OF SCIENCE

Major: Mechanical Engineering

Program of Study Committee:
Atul Kelkar, Major Professor
Shan Hu
Thomas J Rudolphi

The student author, whose presentation of the scholarship herein was approved by the program of study committee, is solely responsible for the content of this thesis. The Graduate College will ensure this thesis is globally accessible and will not permit alterations after a degree is conferred.

Iowa State University

Ames, Iowa

2017

DEDICATION

"I dedicate whatever I possess

to you

my beautiful Iran”

TABLE OF CONTENTS

LIST OF FIGURES

NOMENCLATURE

HR	Helmholtz resonators
f_r	Resonance frequency
k	Spring stiffness
m	Mass
V	Cavity volume
$\rho_\circ$	Fluid density
S	Neck area
L'	Effective length of neck
r_n	Neck radius
P	pressure
C	speed of sound
Q	Resonance sharpness
P_C	Cavity acoustic pressure
z	Impedance
U	Volume velocity.
Z	Acoustic impedance
r	Specific acoustic resistance
x	Specific acoustic reactance
K	Wave number
ω	Angular frequency
M	Acoustic intertance
C'	Acoustical compliance
SPL	Sound pressure level
P_0	Reference pressure
TL	Transmission loss
A_p	Pipe cross sectional area
f	Target frequency
l	Cavity length
λ	Wave length
t	Time
u	Particle velocity
r_c	Cavity radius
A_c	Cavity area
Z_m	Mechanical impedance
H	Porosity
R_a	Airflow resistance
∇T	Incremental thickness
q	Sound source
L	Neck length
X	Displacement
Z_{tp}	Trim panel impedance
Z_s	Surface impedance
F	Force

ACKNOWLEDGMENTS

I would like to thank my committee chair, Prof. Atul Kelkar, and my committee members, Dr. Shan Hu, and Prof. Thomas J Rudolphi for their guidance and support throughout the course of this research.

In addition, I would also like to thank my friends, colleagues, the department faculty and staff for making my time at Iowa State University a wonderful experience. I want to also offer my appreciation to the Iowa Energy Center for providing the funding without which this thesis would not have been possible.

ABSTRACT

Circular concentric Helmholtz Resonators have been extensively studied in various industries whereas Helmholtz resonators with normal incident configuration have not been theoretically, numerically or experimentally analyzed in sufficient depth. These resonators can offer useful acoustic design options when there are several constraints to be considered for example, space limitations, design specifications, materials available etc. For sound insulation on flat surfaces such as windows, Helmholtz Resonators (HRs) need to be normal to the sound pressure waves. This configuration is not extensively addressed in the literature. In this study, the effect of various design parameters such as neck radius, neck length, cavity radius and cavity length on sound transmission loss of HRs has been numerically analyzed and the results are discussed. This study also examines the effect of combining HRs in series and parallel network. Moreover, the effect of adding porous material lining is also explored using three different analysis modules of COMSOL, namely, pressure acoustics, solid mechanics, and poroelastic waves modules. Additionally, a theoretical one-dimensional model for side branch HRs is used to verify the numerical simulation, and the best design is introduced based on the results. Finally, the effect of structural vibrations on sound propagation properties of the system is analyzed and the results are discussed.

CHAPTER 1: INTRODUCTION

Study of sound transmission has always played an important role in different application domains such as automobile, aerospace, household appliances, building architectures, etc. One of the most conspicuous application of sound transmission study is in buildings and home environments where both sound and thermal insulation play an important role in the design of such environments. In recent years there has been push for developing technologies that can offer solutions to reduce not only heat loss through windows but also provide sound insulation. It is estimated that about 3.9 quads of the total energy per year is associated with the heat loss through windows [1].Therefore, windows which are designed to be efficient in terms of both sound and thermal insulation are of high value not only to industry but also to academic society.

Scientists and engineers have struggled during the past few decades to eliminate excessive noise which can affect working and living conditions of people. There are different approaches to control the noise level in the environment. The two broad classification of control approaches are active and passive noise control. Typically, passive noise control techniques are effective at higher frequency ranges such as above 1-3kHz whereas the active noise control is effective in lower frequency ranges, for example up to 1 kHz [2]. The passive techniques of noise control include approaches like: adjusting the sound source to control sound radiation, optimal design of the blockade, material selection considering sound absorption coefficient, etc.

In this study, different Helmholtz Resonators are designed and simulated using COMSOL 5.2a, a commercially available multi-physics modeling and analysis software. Using fundamental physics of HR different configurations and designs are generated by optimizing the configurations of HR for a given target performance. The new designs are simulated and analyzed and comparisons are drawn. Also, as material selection has a significant role in sound insulation, the effect of adding porous materials in sound propagation is also explored using analytical research and numerical simulations.

1.1 Literature Review

There are several different methods to passively control sound transmission, among them optimal design of the blockade, and most benevolent choice of material are popular ones. Ancient Greeks were the first people who started to grasp the rudimentary concept of acoustics that sound is generated from the motion of various parts of human body which is transmitted by the air, and when striking the ear produces the sensation of hearing .The keystones in theoretical side of acoustics were laid early, and the experimental work justified or denied them on the course of history as various scientists such as Biot, Sturm, Boltzman contributed a lot to the experimental studies on acoustics.[3] The greatest impact however was Helmholtz's book entitled "On the Sensation of Tone" published in 1862 in which he discusses resonance theory and theoretically validates Ohm's law.[4] Since Helmholtz cavity resonators were introduced, numerous researchers have studied them. The research of resonators continues because there have been many discordances reported [5] and there are still some aspects of Helmholtz resonators which remain undiscovered. Properties of Helmholtz resonators and their effects on many acoustical performances have been studied by diverse groups of researchers. It has been proven analytically and experimentally that these resonators play a significant role in control of sound. [6] They are frequently used in different industries such as gas turbines, aerospace, vehicles, etc. They can be effectively used in environments in which sound insulation is desired; for example, . home environments, class rooms, hospitals, airports, etc. There has been a significant effort by home building products industry to devise better windows, doors, and wall systems that can offer high levels of sound insulation. Almost all of these designs are focused on passive techniques such as incorporating better materials, tweaking properties of materials, incorporating designs that exploit Helmholtz resonators' properties. However, there are challenges such as the double wall design which has the issue of drop in transmission loss performance that is associated with low resonance frequencies. This has always been a controversial issue and in some cases active noise control methods have been implemented to come up with more robust solutions to the problem.[7,8,9] As work presented in ref [7] tried three different experimental methods of cavity control, panel control and room control to actively control sound transmission through double walls. Also, ref [8] investigated the effect of inserting a loudspeaker to actively control the noise inside the air gap between the double walls analytically, theoretically and experimentally.

Additionally, ref [9] studied feedforward control approach and tested the effect of loudspeaker and microphone placement experimentally to come up with a better solution for active noise control. Despite a large amount of research in active noise control there have been very few realistic solutions that have been implemented in day-to-day home building products. As a result, the work in innovating better passive noise control methods continues alongside of quest for active methods. One possible solution is to use optimally tuned Helmholtz Resonator to control the sound pressure level by increasing the damping factor. Helmholtz resonators have been used in different industries for noise insulation purposes as they don't need a continuous supply of energy and they are highly effective at high frequencies.[10,11,12,13,14] In ref [10] the Helmholtz Resonators (HRs) were tuned to the natural frequencies to achieve a significant acoustic attenuation when they are optimally damped. Additionally, ref [12] discusses the effect of HRs on free vibration, forced vibration and fluid in the enclosure as well as investigating the necessary conditions for noise control. Ref [13] applies the theory of Helmholtz resonators to a blower and both analytically and experimentally solve the problem of varying frequency over time by designing a two-stage auto-tuning resonator which eliminates the problem by minimizing the cost functions of the two major peaks in the frequency domain. Ref [14] experimentally investigates the effects of varying the number of HRs, excitation sources and acoustic field on sound transmission through double glazed windows, whereas ref [15] implements mainly analytical approach to compare different approaches for establishing acoustic characteristics of dual Helmholtz resonators such as lumped parameter method, pressure-velocity matching technique, and boundary-element method. It also develops closed-form expressions for the resonant frequencies and the transmission losses.

As engineers and scientists always want to improve their designs, it became essential for them to look for additional ideas to make the sound absorption performance of the HRs even better. As Matsuhisa and Ren [16] used the method of changing the volume of the cavities to bring about better control over the resonance frequency. Ref [17] used HRs with oscillating volume cavities in combination with electromagnetic shaker and vibrating back plate to both theoretically and experimentally control the acoustic power absorption of the system around the resonance frequency. Dicky and Selamet [18] focused on concentric HRs whose cavities have small length to diameter ratio to develop a one-dimensional closed form solution both for resonance frequencies and transmission losses. In most of the studies regarding HR designs, the length of

the neck of the resonator is significantly smaller than the wavelength of the incident sound, however Doria [19] studied deep cavity, long neck HRs using one dimensional finite element model (linear quadratic shape functions). Also, mathematical expressions of the resonators and analytical solutions for the impedances and resonant frequency are compared to the experimental and numerical results. As changing the characteristics of the neck is much easier than modifying the volume of the cavity, many researchers adopted that method to optimize HR performance. Ingrad [20] and Chanaud [21] scrutinized the effect of different geometries and positions of the HRs on resonance frequencies and sound absorption frequencies. Also, there are several studies regarding changing the structure and the shape of the HRs. Tang [22] improved the sound absorption properties of the HRs by tapering the necks. Also, Selamet and Lee [23] investigated the effect of the length and the shape of the neck on HR performance theoretically, numerically and experimentally. By deriving different two and three dimensional analytical models and comparing the results, the study showed that the shape, length and perforation porosity affects the sound absorption noticeably. Yang et al [24] investigated the effect of the neck material on HRs. They considered ceramics with different perforation diameters to not only gain better acoustic absorption but also improve acoustic impedance. Their study was both experimental and theoretical and the results agreed fairly convincing with each other. Another typical approach for sound insulation is adding porous and fibrous materials to the blockade which has been used a lot throughout the history of sound insulation. Rockwool and fiberglass were used as the traditional materials for sound insulation [25] however limits were set on their employment due to the possible negative health issues. Therefore, some other materials such as polyester fibers were developed instead [26]. Although there are many traditional sound absorbing materials proposed by Lyons [27] which are currently being utilized in multiple layers and potentially heavier materials , new thermal insulating materials came into the view. Aerogel, which is a transparent polymer with thermal conductivity of 13 mW/(m k) can be a cost effective replacement for the traditional sound absorbing materials [28]. As Aerogels have lower speed of sound than air, they can be perfect reflectors of audible sound which makes them ideal barrier materials[29].

Additionally, as theoretical and numerical studies always need to be verified, it is crucial to conduct experimental studies through the course of their research. Based on the aforementioned explanations, there are lots of experimental studies regarding sound propagation

through Helmholtz resonators and porous materials which followed different standards for carrying out their experiments in which [30]and [31]are the most common ones.

1.2 Objectives and Organization of the Thesis

In this study, Helmholtz resonators are investigated to a deeper level through analytical and simulation studies. The governing equations and analytical models of the Helmholtz resonators with different configurations are studied in chapter two. Chapter 3 focuses on the numerical simulation of HRs together with the porous material and a full comparison of the different designs and materials effects on the sound pressure level and sound transmission loss. Chapter 4 is dedicated to results and conclusion and provides direction for future research.

CHAPTER 2: THEORETICAL ANALYSIS

This chapter presents research related to Helmholtz resonator integrated with porous materials to achieve better sound insulation performance. Since early 20th century the time when HRs and their application became mainstream some work in the direction of use of porous materials also began; however, most of the work is still in its infancy and more in-depth investigations are needed. The work presented in this chapter takes a closer look at how combining porous material with HR affects its sound insulation performance. The classical Helmholtz resonator theory is revisited and analytical modeling of side branch HRs is used to validate accuracy of numerical tools used in this work. The effect of porous materials on sound transmission loss is then explored by conducting parametric study using validated numerical simulation tools. Classical Helmholtz Resonator TheoryAs one of the keystones of application of HRs is the fact that if the wavelength of the incident plane wave is long enough to exceed all the dimensions of the HR, then the most effective design in terms of sound insulation can be achieved. Classical HR theories are used a lot to predict the resonance frequency and transmission loss. Therefore, it is critical to fully understand the theory behind HRs.

2.1 Resonant Frequency

The dynamics of the HR can be explained using mass-spring analogy. In this analogy fluid mass in the neck of the HR is representative of a mass and adiabatically compressed volume of HR is representative of a spring. The forcing function like a force in case of mass-spring system is equivalent to an incident pressure in case of HR. Once this mass-spring analogy is established one can apply Newton's laws to obtained governing dynamics (see figure 1) [32].

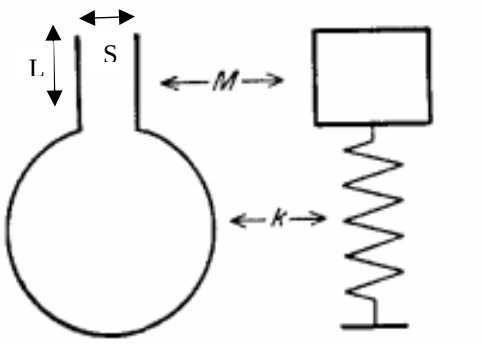

Figure 1. Analogy of a Helmholtz resonator to a spring mass system

The differential equation using the equilibrium of the forces for the unforced system will be:

$$m\ddot{x} + kx = 0 \tag{1}$$

The resonance frequency can be calculated using equation (1) and the solution is:

$$f_r = \frac{1}{2\pi}\sqrt{\frac{k}{m}} \tag{2}$$

If the volume of the cavity is assumed to be V, then the fluid trapped in the neck has a mass of:

$$m = \rho_\circ S L' \tag{3}$$

where, $\rho_\circ$ is the density of the fluid traped in the neck and S is the cross-sectional area of the neck of the HR. L' is longer than L because of radiation-mass loading. L' can be computed as follows:

$$L' = L + 1.7r_{\,n} \qquad (outer\ and\ flanged) \tag{4}$$

$$L' = L + 1.5r_{\,n} \qquad (outer\ and\ unflanged) \tag{5}$$

Where $r_{\,n}$ is the radius of the neck. For determining the stiffness of the system, it is assumed that the air trapped in the neck by an air-tight piston. If the piston is pushed by some distance, the volume of the cavity will change as $\Delta V = -S\Delta l$, as $\frac{\Delta\rho}{\rho} = \frac{-\Delta V}{V} = \frac{S\Delta l}{V}$, then the pressure will be:

$$P = \rho_{\circ} C^2 \frac{\Delta\rho}{\rho} = \rho_{\circ} C^2 \frac{S\Delta l}{V} \tag{6}$$

Where C is speed of sound. As the force F=kx=PS, therefore $k = \frac{PS}{\Delta l}$, then:

$$k = \rho_{\circ} C^2 \frac{S^2}{V} \tag{7}$$

Therefore, the resonance frequency is:

$$f_r = \frac{1}{2\pi}\sqrt{\frac{k}{M}} = \frac{1}{2\pi}\sqrt{\frac{\rho_{\circ} C^2 \frac{S^2}{V}}{\rho_{\circ} S L'}} = \frac{C}{2\pi}\sqrt{\frac{S}{VL'}} \tag{8}$$

Equation (8) reveals that for long wavelengths of the incident pressure, the volume of the cavity, not the shape is effective in the resonance frequencies. Also, the sharpness of the resonance in a HR on the assumption that there are no losses except radiation which resulted in considering the correction factor for the length would be [33]:

$$Q = \frac{P_C}{P} = 2\pi\sqrt{V(\frac{L'}{S})^3} \tag{9}$$

Where P_C is acoustic pressure amplitude inside the cavity. Thus, at the resonant frequency the HR acts as an amplifier with gain Q.

2.2 Acoustic Impedance

One of the ways to study different systems is to convert them into analogous mechanical systems. Another method is also to convert them into electrical systems. For HRs, the motion of the fluid corresponds to the current in an electrical circuit with resistance, capacitance and inductance. The pressure difference is equivalent to voltage in the circuit. And the volume velocity is analogous to the current. Therefore the following equation can be written for impedance:

$$z = \frac{P}{U} \tag{10}$$

where, U is the volume velocity. The acoustic impedance which is the acoustic radiation from the vibrating surface is $denoted\ by\ Z = z/S$. Therefore, the impedance unit would be Pa.s/m^3. Although acoustic impedance can be assumed real for plane waves, it is a complex quantity for standing or diverging waves. In general, acoustic impedance can be written as:

$$z = r + jx \tag{11}$$

where, r is specific acoustic resistance and x is the specific acoustic reactance. If radiation is assumed for the HRs in the same way as open-ended pipe, then:

$$r = \rho_\circ C K^2 \frac{S^2}{2\pi} \tag{12}$$

where, K is the wave number. By considering the differential equation for the displacement of the fluid in the neck, the mechanical impedance of the HR is:

$$Z_m = r + j(\omega m - \frac{k}{\omega}) = \rho_\circ C K^2 \frac{S^2}{2\pi} + j(\omega \rho_\circ S L' + \rho_\circ C^2 \frac{S^2}{V\omega}) \tag{13}$$

where ω is the angular frequency. Also, the acoustic impedance can be derived using the following equation:

$$Z = r + j(\omega M - \frac{1}{\omega C'}) \tag{14}$$

where, M is the acoustic intertance which is equal to $\boldsymbol{M = \frac{m}{S^2} = \rho_\circ \frac{L'}{S}}$ and $\boldsymbol{C'}$ is the acoustical compliance which is derived as $\boldsymbol{C' = \frac{S^2}{k} = \frac{S^2}{\rho_\circ C^2 \frac{S^2}{V}} = \frac{V}{\rho_\circ C^2}}$ and can be substituted in equation (14).

2.3 Sound Pressure Level and Transmission Loss

This parametric study is focused on comparison between effects of different factors such as the cavity size, the neck radius, number of Helmholtz resonators in each panel, and addition of a porous material on sound pressure level and transmission loss.

Acoustic pressure level is the ratio between the pressure of sound and the reference pressure in a logarithmic scale [34]:

$$SPL = 20\log\frac{P}{P_0} = 20\log\frac{ZU}{P_0} \tag{15}$$

P_0 is the reference pressure commonly assumed to be 20μPa. Many researchers tried to find an exact solution for sound transmission loss in Helmholtz resonators which will be discussed in analytical solution section of the thesis. The classical formula for sound transmission loss in a side branch HRs is [35] given by:

$$TL = 10\log[1 + (\frac{\sqrt{\frac{VS}{L'}}/{2A_p}}{f/_{f_r} - f_r/_f})^2] \tag{16}$$

Where, A_p is the cross-sectional area of the main duct and *f* is the target frequency.

2.4 Effect of Helmholtz Resonator Network on Resonant Frequency

One of the methods to enhance the sound absorption performance of Helmholtz resonators is to combine different resonators together. Such a design can be more easily understood if one examines the analogy between the electrical and acoustic system. Different types of HR networks have been studied and introduced by Kinsler et al [33]. In this study the target frequencies are high, therefore the HR configuration mimicking high pass filter is used:

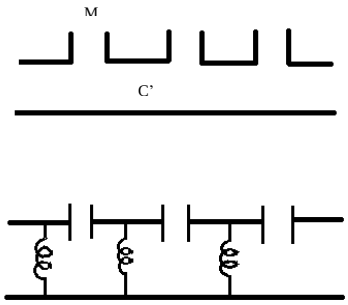

Figure 2: High pass filter design of HRs

The resonant frequency for this HR network is:

$$f_r = \frac{1}{\pi\sqrt{MC'}} \tag{17}$$

2.5 Analytical Helmholtz Resonator Model

As Helmholtz resonators have been used a lot in various types of research and experiments showed noteworthy deviation from the theoretical approach, researchers struggled to use analytical approach to discover more exact formulations for the resonant frequency and transmission loss in Helmholtz Resonators.

2.5.1 Resonant Frequency

The equations of acoustic transmission are solved for the mass loaded neck and infinite impedance is considered as boundary conditions at solid end (see Figure 3). Using the equations for left-moving and right-moving plane waves we have [5]:

$$p_- = \alpha \exp[-j(\omega t + Kx)] \tag{18}$$

$$p_+ = \beta \exp[-j(\omega t - Kx)] \tag{19}$$

Also, as the volume velocities are $U_+ = P_+/(\frac{\rho_0 C}{A_c})$ and $U_- = -P_-/(\frac{\rho_0 C}{A_c})$, therefore:

$$Z = \frac{p_+ + p_-}{U_+ + U_-} = \left(\frac{\rho_0 C}{A_c}\right) * \frac{p_+ + p_-}{p_+ - p_-} \tag{20}$$

where, A_c is the cavity cross sectional area. If the above equation is evaluated at x=0 and x=l and the boundary condition of rigid wall is applied at x=0, it will result in infinite impedance and$Z_0 = j\frac{\rho_0 c}{A_v}\cot Kl$. Also, if the impedance at l is modeled by a lumped mass in the neck we have:

$$Z_l = j\omega\frac{m}{S^2} = jKc\frac{\rho_0 SL'}{S^2} = jKl\frac{\rho_0 CL'}{lS} \tag{21}$$

Therefore, we have:

$$\cot Kl = \frac{L'A_c}{SL}Kl \tag{22}$$

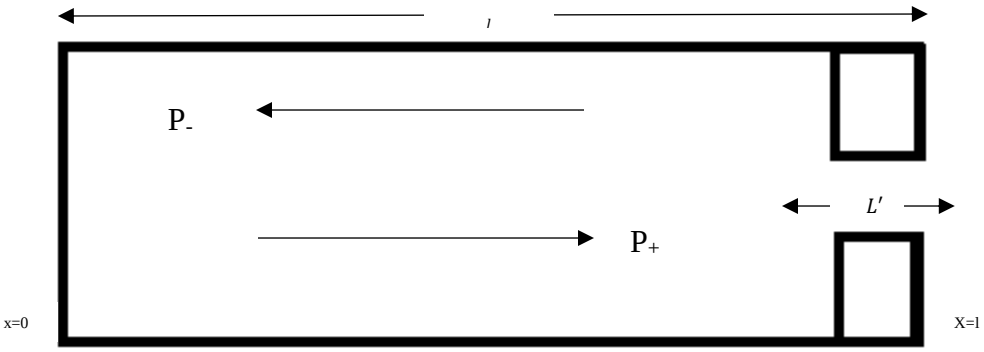

Figure 3 Side view of a cylindrical Helmholtz Resonator

If both $\frac{L'A}{SL}Kl$ and $\cot Kl$ be plotted, the first intersections of these to plots which is the Helmholtz frequency can be found as, $Kl = \omega l/c$. If the closed form approach is applied to find the left-hand side of equation (22), then:

$$\cot Kl = \frac{1}{Kl} - \frac{1}{3}Kl - \frac{1}{45}(Kl)^2 - \cdots \tag{23}$$

The classical formula for HR resonant frequency is achieved using the first term in equation (23), whereas it deviates from the classical formula in $l > \frac{\lambda}{16}$ therefore the revised HR resonant frequency formula can be derived by holding both terms from equation (23) which results in:

$$f_r = \frac{C}{2\pi}\sqrt{\frac{S}{VL' + \frac{1}{3}l^2 S}} \tag{24}$$

2.5.2 Acoustic Impedance

To achieve a more exact solution for different acoustic variables than those of the classic formula, one or multi-dimensional analytical approaches can be used. Although the multidimensional approach is notably more powerful than the one dimensional one where $(\mathrm{l} - \mathrm{L})/2r_c$ is of order 0.1 to 1, [36] the one dimensional one still brings about much more precise solutions than the classical formulation. By considering a planar wave propagation and a radial wave motion in the neck the wave equation can be written as:

$$\frac{1}{r}\frac{\partial}{\partial r}\left(r\frac{\partial p}{\partial r}\right) = \frac{1}{C^2}\frac{\partial^2 p}{\partial t^2} \tag{25}$$

Considering the harmonic dependence:

$$p(r,t) = P(r)e^{i\omega t} \tag{26}$$

By separation of variables, the pressure amplitude can be derived as:

$$P(r) = C_1 H_0^{(1)}(Kr) + C_2 H_0^{(2)}(Kr) \tag{27}$$

Where C_1 and C_2 are respectively related to the oscillation amplitudes of inward and outward moving waves, also $H_0^{(1)}$ and $H_0^{(2)}$ are Bessel functions of the third kind, of order 0 and types 1 and two respectively which can be denoted as $H^{(1)} = J + iY$ and $H^{(2)} = J - iY$ with J being the Bessel function of the first kind and Y being the Bessel function of the second kind. As the momentum equation holds:

$$\frac{\partial u}{\partial t} = -\frac{1}{\rho_0}\nabla p \tag{28}$$

Coupling equation (28) with the harmonic relationship:

$$u(r,t) = U(r)e^{i\omega t} \tag{29}$$

Therefor by applying equation (28) to equations (26) and (27):

$$U(r) = -\frac{i}{\rho_0 C}[C_1 H_1^{(1)}(Kr) + C_2 H_1^{(2)}(Kr)] \tag{30}$$

If a cylindrical junction is assumed at the intersection of the neck and the cavity, u=0 at the junction with r=r_c, Therefore:

$$Z_v = P(r)/U(r) = i\rho_0 C\left[\frac{H_0^{(1)}(Kr_n) - \frac{H_1^{(1)}(Kr_c)}{H_1^{(2)}(Kr_c)} H_0^{(1)}(Kr_n)}{H_1^{(1)}(Kr_n) - \frac{H_1^{(1)}(Kr_c)}{H_1^{(2)}(Kr_c)} H_1^{(2)}(Kr_n)}\right] \tag{31}$$

where, r_n is the neck radius and r_c is the cavity radius.

2.5.3 Transmission Loss

Based on equations (27), (30) transmission loss for side-branch Helmholtz Resonators and for low $(l - L)/2r_c$ can be calculated as:

$$TL = 10\log[1 + \frac{S}{A_p}[\frac{1 + iXtanKL'}{X + itanKL'}]^2 \tag{32}$$

where, $X = \frac{Z_c}{\rho_0 C}(\frac{r_n}{2*(l-L)})$, and A_p is the main pipe area. But, as $(l - L)/2r_c$ increases, the planar wave propagation begins to weaken, therefore the closed-form approach using ref [31], for planar wave propagation, the general form of:

$$TL = 10\log_{10}\left|\frac{C_{+i}}{C_{+tr}}\right|^2 \tag{33}$$

C_{+i} is the magnitude of the incident pressure and C_{+tr} is the magnitude of transmitted pressure. Using the one-dimensional theory and neglecting viscous effects:

$$TL = 10\log_{10}\left|1 + \frac{S}{2A_p}[\frac{1 + \varphi + (\varphi - 1)e^{-2iKL'}}{1 + \varphi - (\varphi - 1)e^{-2iKL'}}]\right|^2 \tag{34}$$

where, $\varphi = \frac{A_c}{A_n}(\frac{e^{2iKl}-1}{e^{2iKl}+1})$ and A_c is the cavity area. If the above equation be converted to the trigonometric structure, then:

$$TL = 10\log_{10}\left[1 + (\frac{S}{2A_p}\left[\frac{\tan KL' + \left({}^{A_c}/_{S}\right)\tan Kl}{1 - \left({}^{A_c}/_{S}\right)\tan Kl \tan KL'}\right])^2\right] \quad (35)$$

There are several ways to make equation (35) even simpler, by assuming $S = A_c$ or ${}^{A_c}/_{S}$ approaching zero. If the volume is fixed and both L' and l approach to zero, then equation (35) will be equal to equation (16).

2.5.4 Effect of Helmholtz Resonator Network on Resonant Frequency

To enhance the sound absorption performance of the HRs in higher frequencies, Helmholtz Resonator arrays can be implemented. As in ref [37] the effect of using HR arrays on sound transmission loss was scrutinized analytically, numerically and experimentally. Based on their findings, the resonant frequency of the HR network is expected to be close to the mean resonance frequency of each single HR. The transmission loss can be calculated as:

$$TL = 20\log_{10}[\frac{Z_1\rho_0 C}{2Z_1}(\frac{p_1}{p_2}.\frac{p_2}{p_3}.\frac{p_3}{p_4}...\frac{p_n}{p_t})] \quad (36)$$

where, Z_1 is the source impedance, p_1 is the summation of incident and reflected pressures and p_t is the transmitted sound pressure. $\frac{p_n}{p_{n+1}}$is the pressure ratio and can be calculated if the characteristic and the termination impedance for each element is known. Equations for the pressure ratio for different panels can be found in ref [38] Also, it should be noted that the termination impedance of each element is the incident impedance of its adjacent element. The input impedance for a single HR j is calculated as :

$$Z_j = r_j + i(\omega M - \frac{1}{\omega C'}) \quad (37)$$

Where:

$$r_j = R_0 + r_1\bar{U} \quad (38)$$

$$R_0 = 2(\frac{\sqrt{\pi\mu\rho f}}{\pi(r_n)^2})(2 + \frac{L}{r_n})$$

(39)

Where the root mean square volume velocity is:

$$\bar{U} = \sqrt{\sum_{q} \frac{P_q^2}{R_q^2 + X_q^2}} \tag{40}$$

where, P_q, R_q, and X_q are the root mean square pressure, resistance and reactance respectively in the frequency spectrum with the increment of q. For a distinct frequency equation (40) will be $\bar{U} = \frac{P}{\sqrt{R^2+X^2}} = \frac{P}{|Z|}$. For a network of N resonators arranged in parallel configuration the impedance is given by:

$$\frac{1}{Z} = \sum_{j=1}^{N} \frac{1}{Z_j} \tag{41}$$

Therefore, the impedance is $z = SZ$ in rayls and can be used in surface impedance equation which is:

$$Z_S = zZ_{tp}/(z + Z_{tp}) \tag{42}$$

where, $Z_{tp} = \rho_0 C - i\omega a$, and a is the density of the resonator and trim panel.

2.6 Effect of Porous Materials on Helmholtz Resonators

Sound absorptive materials are the ones which scale down the acoustic energy of the sound wave that passes through them. They can be either porous, fibrous or in other complex forms. The mechanism of an absorber is converting the mechanical motion of the air into heat. As a result the power of the reflected noise will diminish. They neutralize the effect of unwanted reflections by rigid interior surfaces. Based on the target frequency spectra, different materials can be chosen with regards to different characteristics explained below [39].

2.6.1 Porosity

The size, quantity and type of the pores are the factors that should be borne in mind while studying the effect of porous material on sound transmission. The sound wave should penetrate

in the porous material in order to bring about sound dissipation by friction. Therefore, the volume of pores should be enough to allow for sound insulation. The definition of porosity is:

$$Porosity\ H = \frac{V_a}{V_m} \tag{43}$$

where, $V_a$is the volume of air trapped in the voids of the porous material, and V_m is the total volume of the material. Based on the above explanations porosity is directly proportional to the transmission loss and sound absorption coefficient.

2.6.2 Tortuosity

By definition, tortuosity is a measure of elongation of the path through the pores compared to the thickness of the material which interprets the effect of material structure on the acoustical behavior of the porous material. Different researchers have studied the effect of this measure on sound absorption and reported that it mostly affects the location of quarter length peaks. Also, some other researchers believed that it significantly affects the high frequency behavior of the material.

2.6.3 Airflow Resistance

Between all the acoustical properties of materials, one of the most important one is airflow resistance which governs the propagation constant and the characteristic impedance which are significant acoustic properties of materials. Generally, when sound goes through a porous material, its amplitude reduces due to the friction in the tortuous passage. As a result, this energy is converted to heat. The friction is depicted by the resistance of the material to airflow and calculated by:

$$R_a = \frac{\nabla p}{\nabla T u} \tag{43}$$

where, u is the particle velocity, ∇p is sound pressure differential over the material thickness and in the same direction as particle velocity, and ∇T is the incremental thickness. Based on the equation, the more the airflow resistance, the more the pressure difference, sound absorption coefficient and transmission loss. Also, this measure is inversely proportional to the square pore size of a given porous material and to the fiber diameter.

2.6.4 Thickness

There have been numerous studies on the thickness effect on sound absorption of a porous material which concluded that the thickness of the porous material has direct relationship with the sound absorption at low frequencies. The most competent sound insulation is achieved when the wavelength of the incident sound is ten times of the thickness of the material. Another study showed that the thickness adversely affects the sound transmission loss at higher frequencies.

2.6.5 Surface Impedance

Based on equation (11), the surface impedance rises directly with flow resistance, which results in a great amount of reflection, and less absorption capability. On the other hand, the more the acoustic resistivity of a material, the higher the dissipation due to friction. Additionally, the whole concept is frequency dependent. Therefore, it will be hard to theorize the effect of surface impedance of a porous material on sound insulation.

2.6.6 Density

Density has always played an important role is considered as the effective parameter in acoustics. As the cost of a porous material is always a function of its density, it is always a tradeoff whether to add a dense porous material to the system or not. It has been observed that less dense materials perform better at low frequencies (500 Hz) and denser structures tend to absorb more at high frequencies (above 2000)

2.6.7 Position of sound absorbing material

One of the mostly studied variables in sound insulation and noise control using absorptive material is their position. It has been concluded that in case of using diverse absorbers, all three axial modes (vertical, transverse and longitudinal) should come under the absorptive material's influence. Therefore, it is better to attach them on ends, sides and ceilings. Also, for shapes that have corners it is better to attach them to corners to avoid reflection. Additionally, untreated surfaces shouldn't preferably face each other.

CHAPTER 3: NUMERICAL ANALYSIS

Based on the explanations in the previous chapter, the analytical equations for different features of Helmholtz resonators do not match the experimental and numerical results completely in most of the published studies. Also, there are lots of discrepancies being observed in this field as different papers suggest different formulas and equations for acoustic properties of HRs. Therefore, both numerical and experimental study will be necessary to verify the theory which was suggested.

As it was discussed in the previous chapters, there are many factors that affect the sound pressure level and therefore, sound transmission loss. Based on the analytical results from chapter two the effective design variables are r_n, L', l and r_c . Other possible ways of enhancing the sound insulation performance would be using HR networks and adding a porous material to the designed Helmholtz resonator.

In this chapter of the study, the numerical study on differently designed HRs is performed to investigate the effect of the above parameters using COMSOL 5.2a implementing Acoustic Structure Interaction package which couples Acoustic and Structure module. Also, for modeling the porous material the poroelasticity module is coupled with the previous ones to achieve more accurate results. The simulations are explained in the following paragraphs and the most conspicuous concerns are being addressed. The results and comparison with experimental and analytical studies are explained in the following chapters.

3.1 Acoustic Structure Interaction

When a disturbance in a fluid carrying acoustic pressure waves is caused by a vibrating object, sound is generated. This pressure wave in the system will also affect the structure which will consequently lead to a variation in the acoustic pressure wave. This interaction- mostly referred to as acoustic-structure interaction, is bidirectional, in spite of the fact that one of the interactions overweighs the power of the other one most of the times, in some applications both the vibrations of the solid structure and the acoustic pressure variation is noteworthy enough to

be taken into account which results in the necessity of Acoustic-structure-interaction module for computing the transmission loss and other features of HRs.

3.1.1 Main Model Definition

In accordance with the purpose of this study, which was to investigate the performance of HRs in window application, the material selection is modified to satisfy the transparency need. Therefore, the material used in this study is acrylic plastic. Also, due to the limitation on experimental setup, the actual model dimensions are small scale compared to the real world problem. Additionally, different patterns are studied numerically for the sake of comprehensiveness of the study, and the results of the investigations are discussed in the next two chapters.

The main model consists of two 5 inch (0.127 m) radius, 0.125 inch thick (0.003175) acrylic plates, with a 0.5 inch (0.0127 m) radius hole located in the center of the front one which acts as the neck of the HR or the mass in the spring mass system analogy. The airgap-which determines the cavity volume- is the variable that acts as the spring in the aforementioned analogy and can be adjusted to achieve a certain target frequency based on equation (8). The incident sound pressure is assumed to be 100 dB which equals the sound pressure level of a circular saw and the source is 1 inch (0.0254 m) away from the front acrylic. The general schematic of the main model is shown in figure 4:

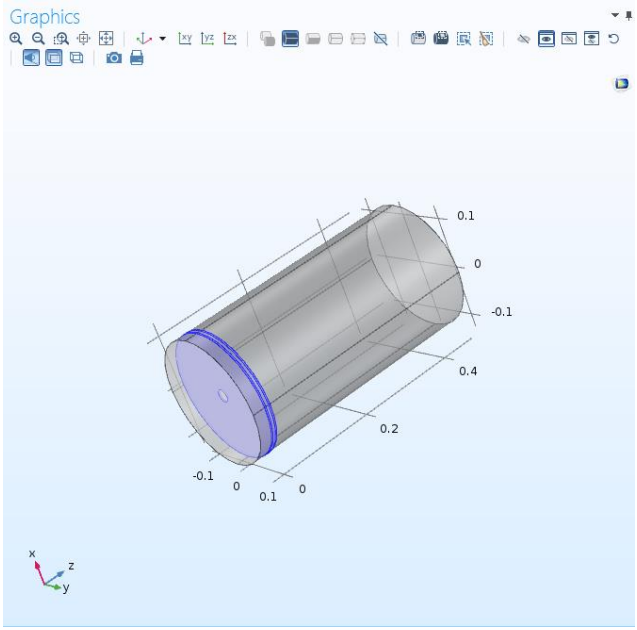

Figure 4Main model schematic

The purple areas in the above figure are the acrylic plates and the grey areas are the air domain. By a further look at Figure 5, the HR geometry is more evident.

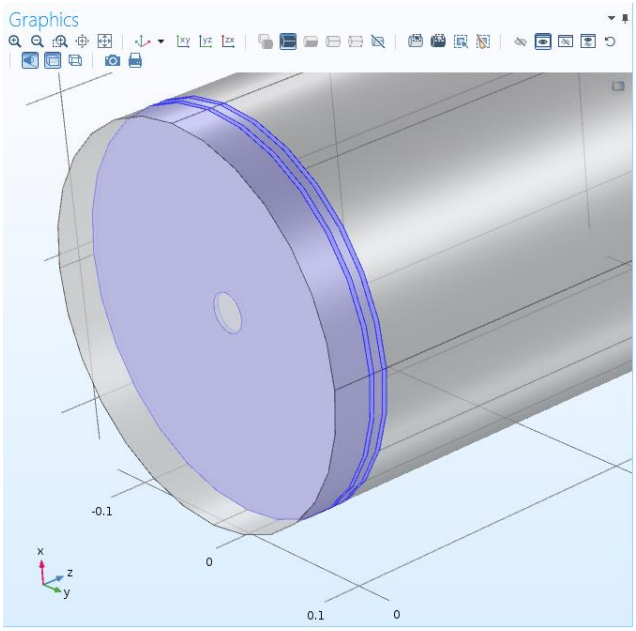

Figure 5: HR geometry in the main model

Main Model Geometry	
Variable	Value
r_n	0.0127
L'	0.0248
r_c	0.127
l	0.006
f_r	449.14

Figure 6: Effective Variables of the Main HR

As it is observable in the picture, this model consists of only one HR which is located at the center of the geometry. The front panel is influenced by the acoustic pressure. This model is capable of computing the frequency response of the structure and feeding the necessary information back to the acoustics domain which results in a comprehensive wave pattern analysis. For this purpose, the two physics interfaces which are pressure acoustic and solid mechanics, frequency domain Multiphysics and acoustic-structure boundary should be coupled. As a result, the main model calculates the stresses and the displacement due to the acoustic

pressure on the solid structure (acrylic plates) and using the normal acceleration concept in the acoustic field boundary secures the continuity.

3.1.2 Domain Equation

The pressure acoustics domain models the sound waves using Helmholtz equation for sound pressure [40]

$$\nabla.\left(\frac{-1}{\rho}\nabla p\right)-\frac{\omega^2 p}{c^2\rho}=0 \tag{44}$$

where, $p=p_0e^{i\omega t}$. To calculate different acoustic and structure properties, such as sound pressure level, strain and stress Linear Elastic Model feature in conjunction with pressure acoustics module should be used.

3.1.3 Boundary Conditions

In the acoustics module there are 3 boundary conditions that are applied to the problem. The first one is the sound hard boundary at which the normal component of the acceleration is zero [40] in other words, the structure will not be influenced by the pressure of the sound, but its existence inevitably affects the distribution of sound:

$$-\mathrm{n}.\left(\frac{-1}{\rho}(\nabla p-q)\right)=0 \tag{45}$$

Where q is the sound source which can be either dipole or monopole sound. Another used boundary condition is plane wave radiation which permits the outgoing sound wave to reflect the least amount possible. The wave radiation has diverse types. It can be plane, cylindrical or spherical. The plane wave one is suited to far field boundaries which is applied to the model using the following equation:

$$-\mathrm{n}.\left(\frac{-1}{\rho}(\nabla p_t-q)\right)+iK\frac{P}{\rho}=iK\frac{P_i}{\rho}+n.(\frac{\nabla p_i}{\rho}) \tag{46}$$

where, p_t is the transmitted sound pressure and P_i is the incident sound pressure. The third boundary condition which is used in acoustic pressure domain is the incident pressure which is 2 Pascals (100 dB) for the main model. Based on equation (16) transmission loss is not a function of the incident pressure. Therefore, it shouldn't affect the results. Additionally, there are two

boundary conditions used in the solid mechanics domain. The fixed constraint is applied to both of the acrylic plate walls as they are going to be fixed in the real world problem as well. Also, the free constraint is applied to all the fluid (air) domain. Moreover, the Multiphysics domain which couples the acoustics and fluid domains is fulfilled by applying the acoustic-structure boundary feature. It sets the boundary load F on the solid structure as:

$$\mathrm{F} = -n_s p \tag{47}$$

where n_s is the unit normal vector observed from inside of the structure (acrylic domain in our study). Also, on the acoustic (fluid) side of the simulation the normal acceleration of the structure would be equal to the normal acceleration experienced by the fluid. Corresponding mathematical expression is given by:

$$-\mathrm{n}_a.\left(\frac{-1}{\rho}\nabla p + q\right) = \mathrm{a}_n \tag{48}$$

where n_a is the unit normal vector observed from inside of the acoustic field (fluid (air) domain in our study), and the normal acceleration $\mathrm{a}_n = (n_a.u)\omega^2$, in which u is the computed displacement vector from the solid domain.

3.1.4 Mesh Specification

The main challenge in finite element simulation study is the creation of mesh to yield accurate results. Meshing is very important aspect of finite element analysis especially in this multi-physics problem. If the meshes are not fine enough to allow short edges and thin regions to be resolved perfectly, the simulation will not yield right results. For gaining further insight into mesh properties the *Measure* feature of COMSOL is used. This feature can allow users to examine mesh size, length of the mesh, mesh type, boundary layers, distribution, scale and few other parameters.

For 3-D meshing the domain is discretized using different types of elements such as pyramid, prism, tetrahedral, and hexahedral to achieve the resolution needed at the boundaries, edges and vertices. The meshing problems can be minimized by understanding the underlying physics of the problem and then choosing the meshing by using free or structured meshing techniques in

which the mesh size, element size, curvatures, mesh distribution, and other meshing parameters could be controlled.

Because of the simplicity of the current model, the mesh applied was a free tetrahedral fine mesh with the element size range between 0.005 and 0.04 m with average element growth rate of 1.993, curvature factor of 0.5 and 0.6 resolutions of narrow regions as shown in figure 7:

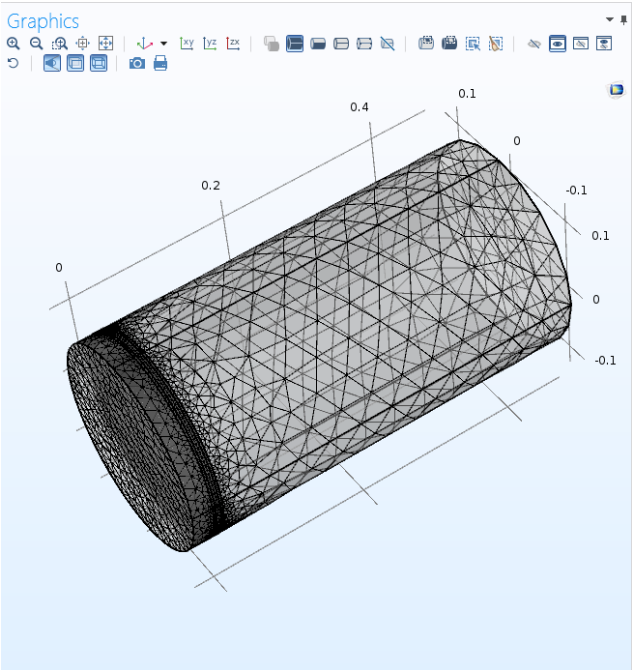

Figure 7: Mesh on the main model

3.1.5 Main Model Simulation and Analysis

As mentioned previously, the purpose of this study was to compare the sound pressure level and the sound transmission loss of the prototype system with varying HR configurations. The simulation study was conducted over a wide range of incident wave frequencies. The frequency range considered was 200 to 800 Hz with a step size of 50 Hz. The simulation results were obtained for acoustic pressure distribution, sound pressure level distribution, and stress . The sound pressure level spectrum for 500 Hz is shown in fig 8:

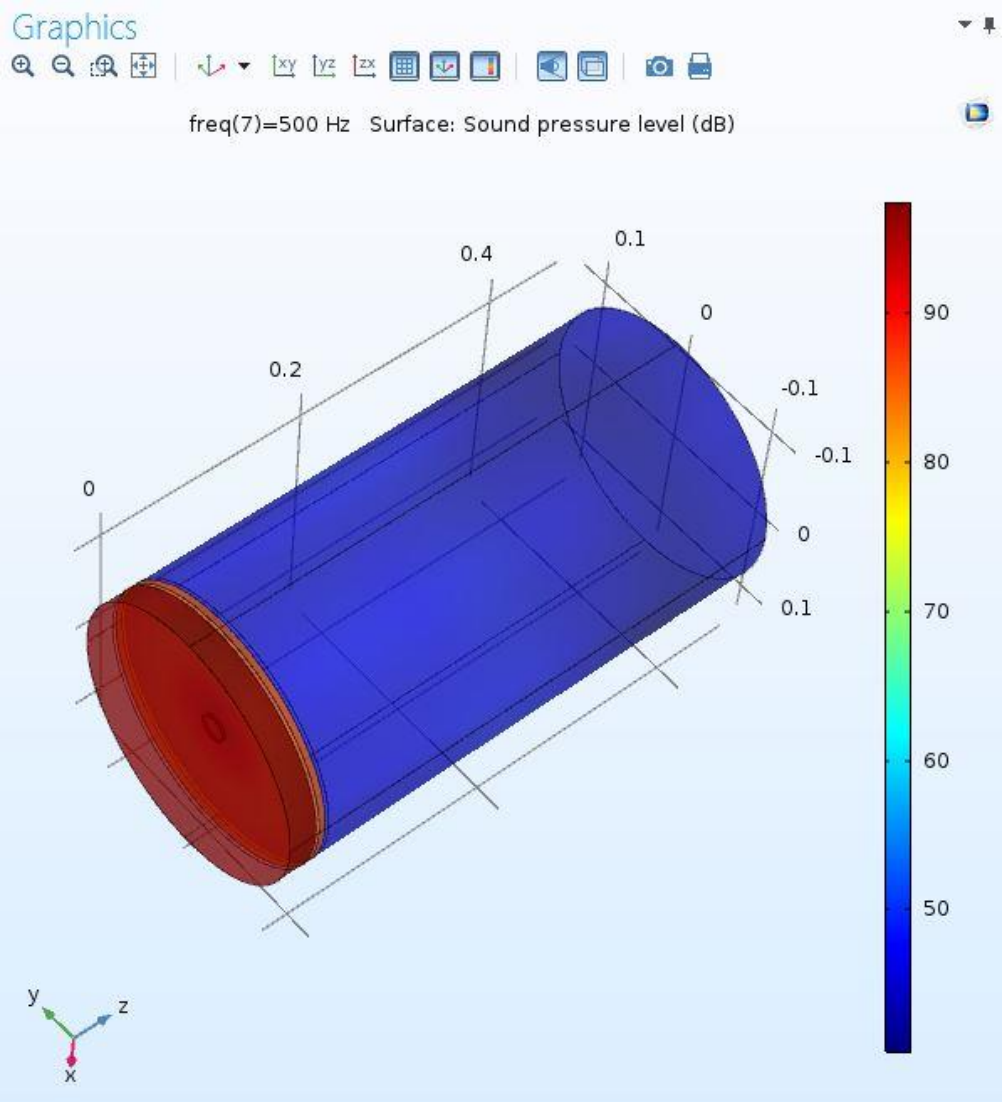

Figure 8: Sound Pressure Level at 500 Hz

As shown above, there is a significant drop in sound pressure level when air passes the HR. The quality and amount of sound insulation will be discussed in detail in the Result and Conclusion chapter. Also, the stress plot is shown in fig 9, in which the numbers in the right hand side of the picture only shows the scale of the von Mises stress not the actual measure of it:

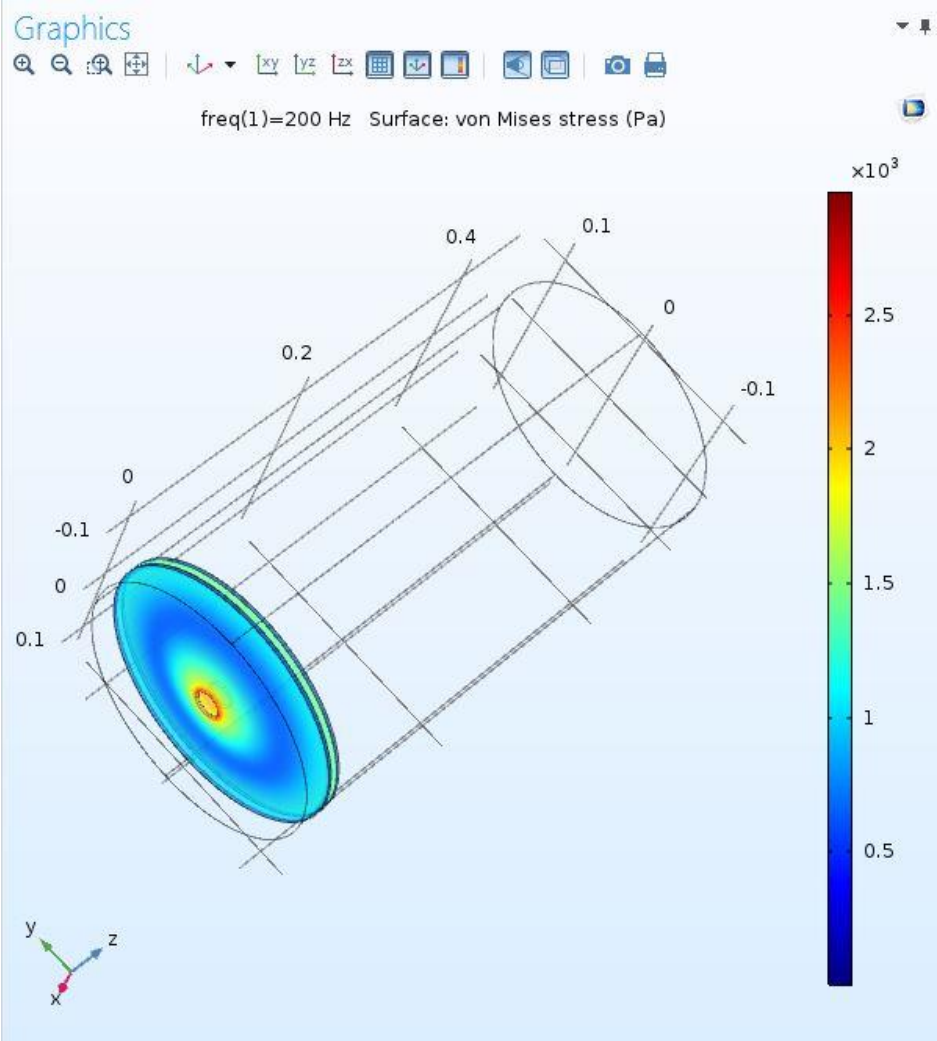

Figure 9: Stress Plot of the Main Model

3.1.6 The Effect of Neck Radius on Sound Transmission Loss

As discussed previously, there are different factors that affect the resonant frequency and the transmission loss of Helmholtz resonators. Based on equations (8) and (16) one of these factors is, $S = \pi(r_n)^2$. To investigate the effect of neck radius two different neck radius sizes were used. In one case the radius was doubled the nominal size and other case it was half the size. The simulation results are shown in figs 10 through12.

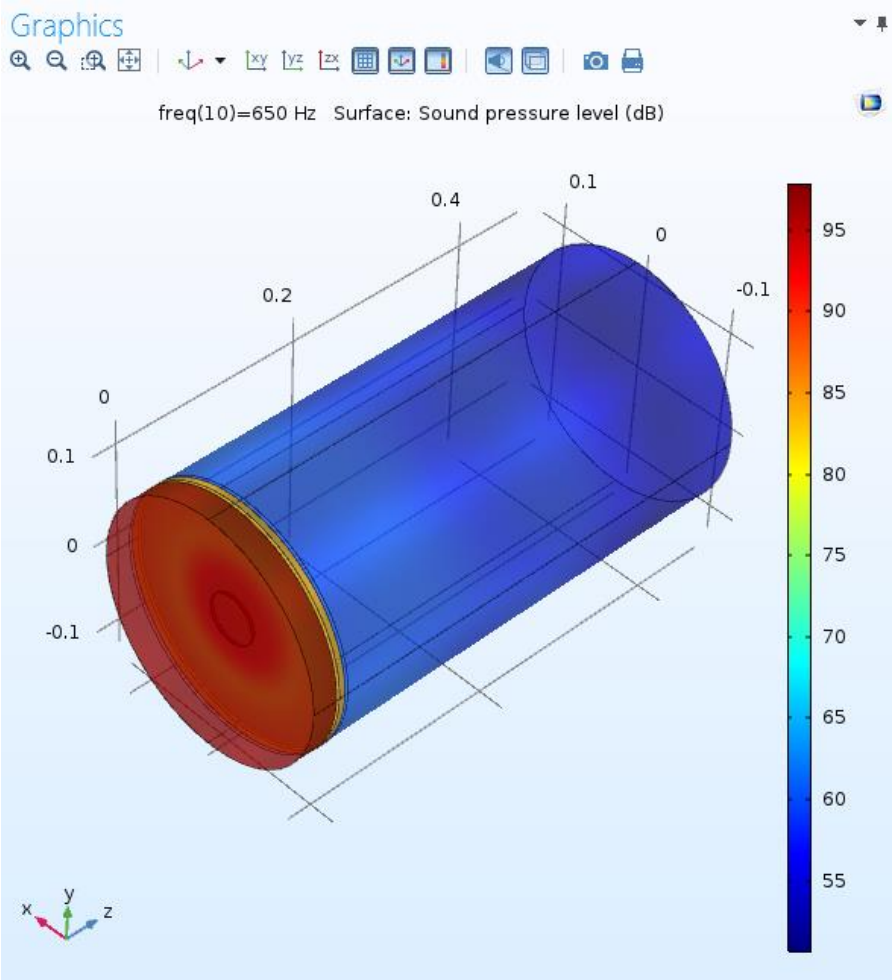

Figure 10 Doubled Neck radius Model SPL

Main Model Geometry		Model 2 Geometry		Model 3 Geometry	
Variable	Value	Variable	Value	Variable	Value
r_n	0.0127	r_n	0.0254	r_n	0.00635
L'	0.0248	L'	0.0464	L'	0.014
r_c	0.127	r_c	0.127	r_c	0.127
l	0.006	l	0.006	l	0.006
f_r	449.14	f_r	617	f_r	299

Figure 11: Neck Radius Comparison Models Geometries

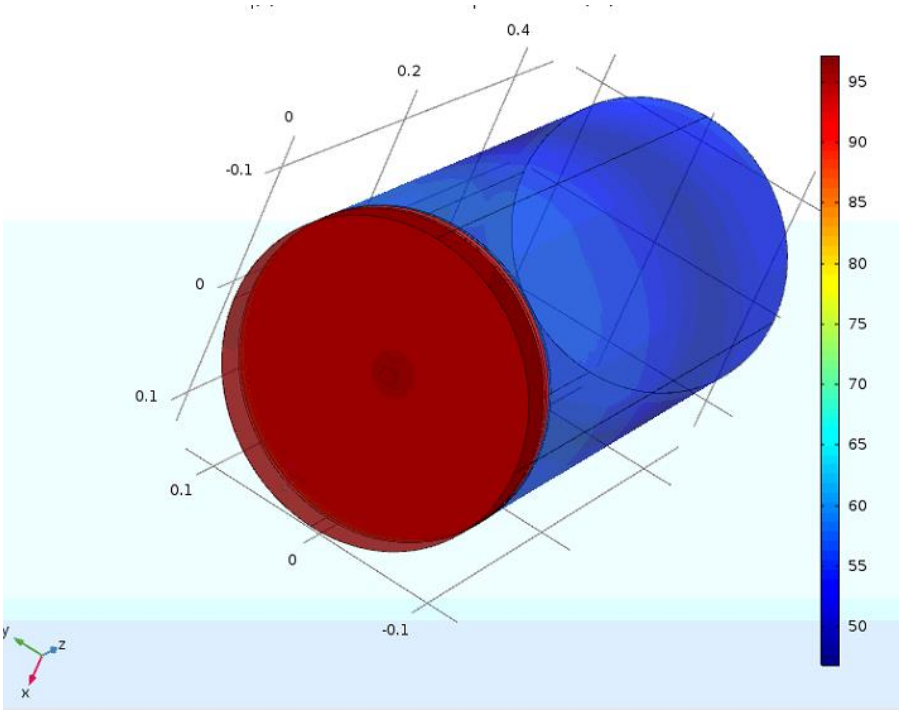

Figure 12: SPL of the Model with the Reduced Neck Radius

Based on the executed simulation, as well as the theoretical equations from chapter two, the neck radius effect on transmission loss is shown in fig 13:

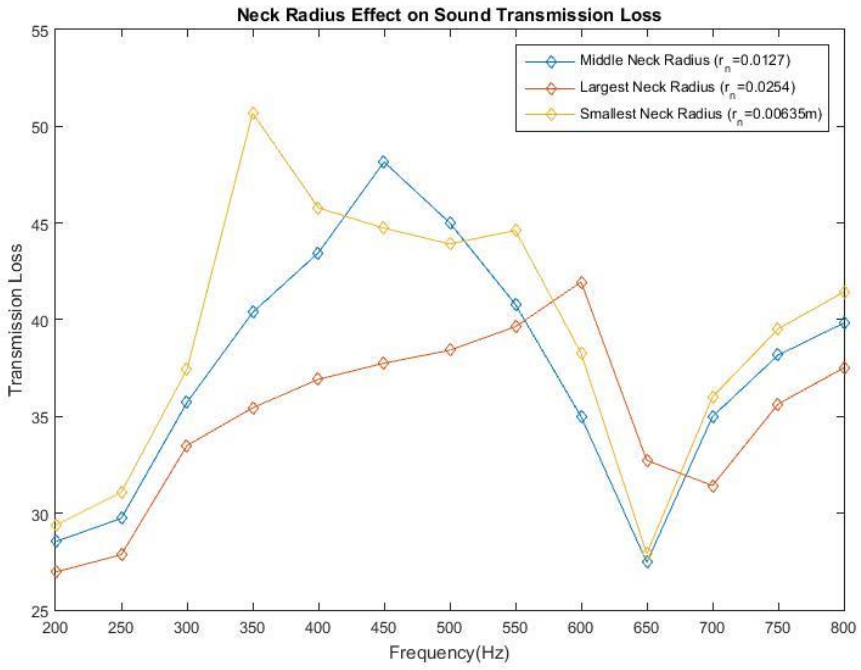

Figure 13: Neck Radius effect on Transmission Loss Plot

3.1.7 The Effect of Effective Neck Length on Sound Transmission Loss

Another factor affecting sound transmission loss is the neck length which affects the factor $V = \pi(r_v^2) * l$ in both equations (8) and (16). Similar to the procedure in the previous section, two different effective neck length sizes were used for comparison. The size was doubled in one case and reduced to 88% of its original value in the second case. The effective variables of the three compared models are shown in fig 15:

Main Model Geometry		Model 4 Geometry		Model 5 Geometry	
Variable	Value	Variable	Value	Variable	Value
r_n	0.0127	r_n	0.0127	r_n	0.0127
L'	0.0248	L'	0.0496	L'	0.022
r_c	0.127	r_c	0.127	r_c	0.127
l	0.006	l	0.006	l	0.006
f_r	449.14	f_r	312	f_r	471.88

Figure 14: Neck Length Comparison Models Geometries

The simulation for the augmented neck length is shown in fig 16:

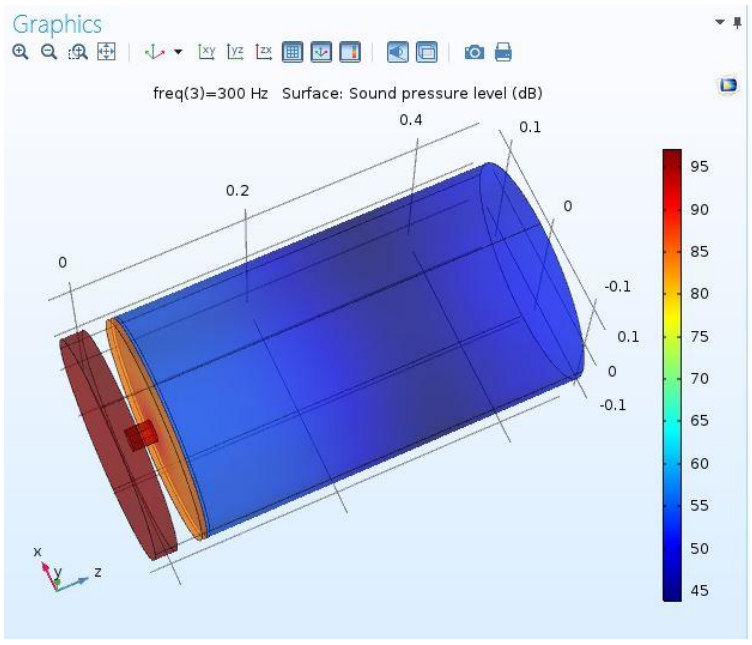

Figure 15: Doubled Neck Length Model SPL

Additionally, the simulation for the reduced neck length is shown in fig 17:

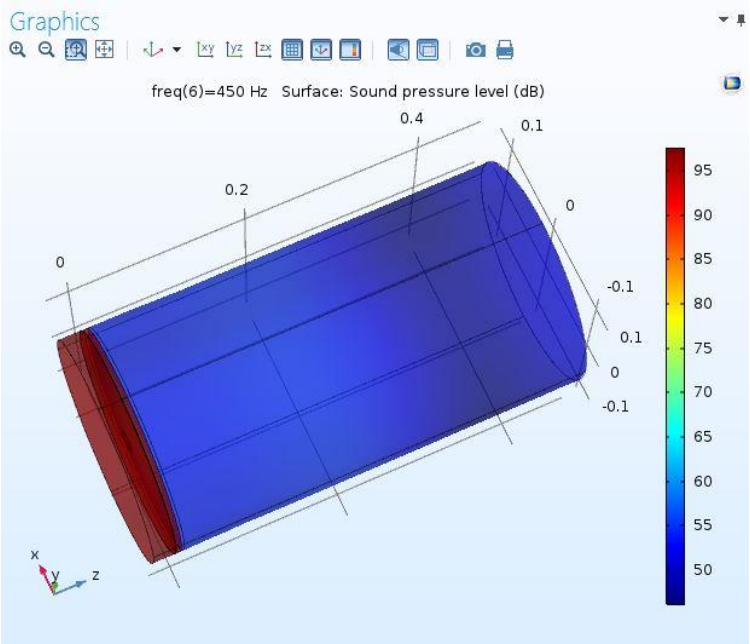

Figure 16: SPL of the Model with the Reduced Neck Length

Based on the sound pressure level data from the rendered simulation, the effective neck length impact on sound transmission loss is given in Fig. 17.

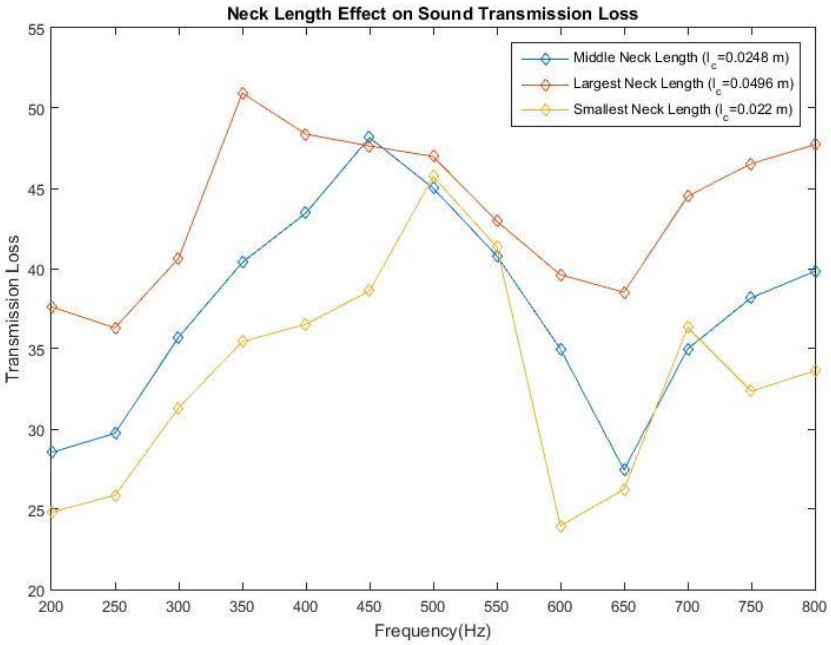

Figure 17: Neck Length Effect on Transmission Loss Plot

3.1.8 The Effect of Cavity Radius on Sound Transmission Loss

Another variable that has effect on both resonance frequency and the transmission loss is the cavity radius. This factor affects cavity volume $V = \pi(r_v^2) * l$ (see equations (8) and (16)) and the resonant frequency; and, as a result, the transmission loss. Similar to the procedure in the previous section, the two cavity radii were chosen for parametric analysis. The results are shown in fig 19:

Main Model Geometry		Model 6 Geometry		Model 7 Geometry	
Variable	Value	Variable	Value	Variable	Value
r_n	0.0127	r_n	0.0127	r_n	0.0127
L'	0.0248	L'	0.0248	L'	0.0248
r_c	0.127	r_c	0.254	r_c	0.0635
l	0.006	l	0.006	l	0.006
f_r	449.14	f_r	223.97	f_r	898.28

Figure 18: Cavity Radius Comparison Models Geometries

The sound pressure level of the large cavity radius model at 250 Hz is shown in figure 20:

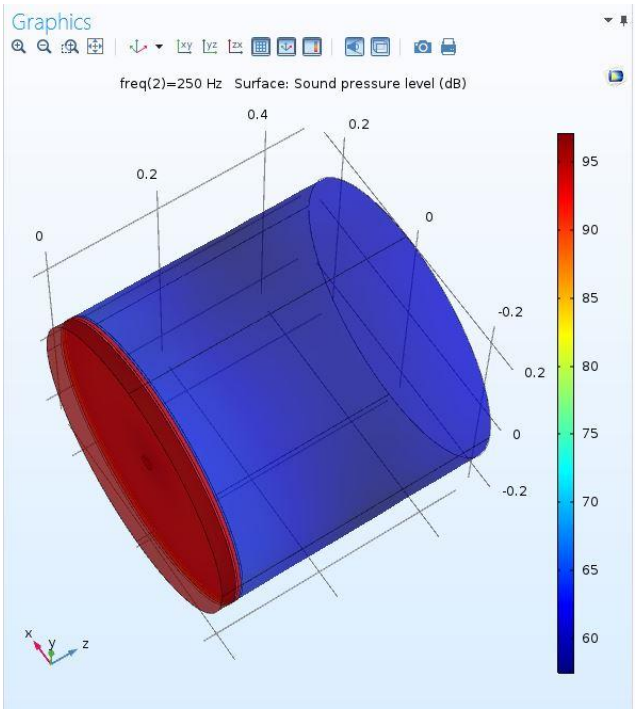

Figure 19: Doubled Cavity Radius Model SPL

The SPL of the small cavity model is depicted in figure 21:

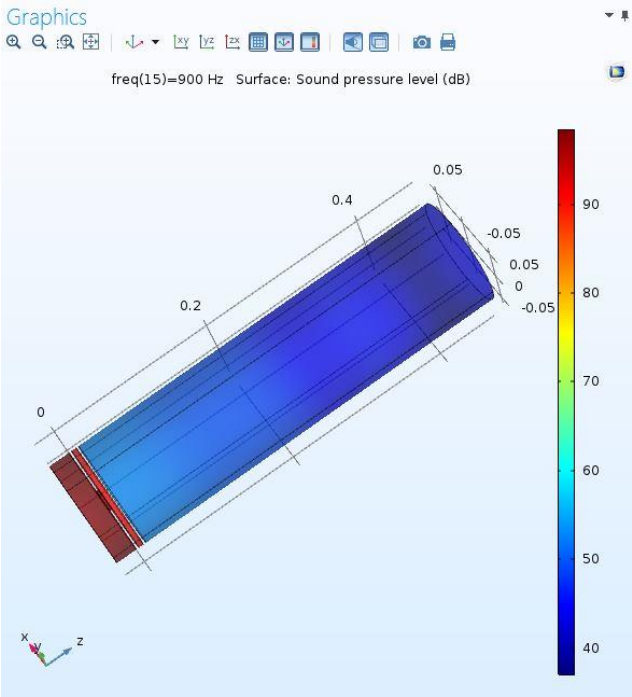

Figure 20: SPL of the Model with the Reduced Cavity Radius

Based on the data from the acoustic structure interaction study, the effect of the cavity volume (or cavity radius) could be summarized in fig. 21:

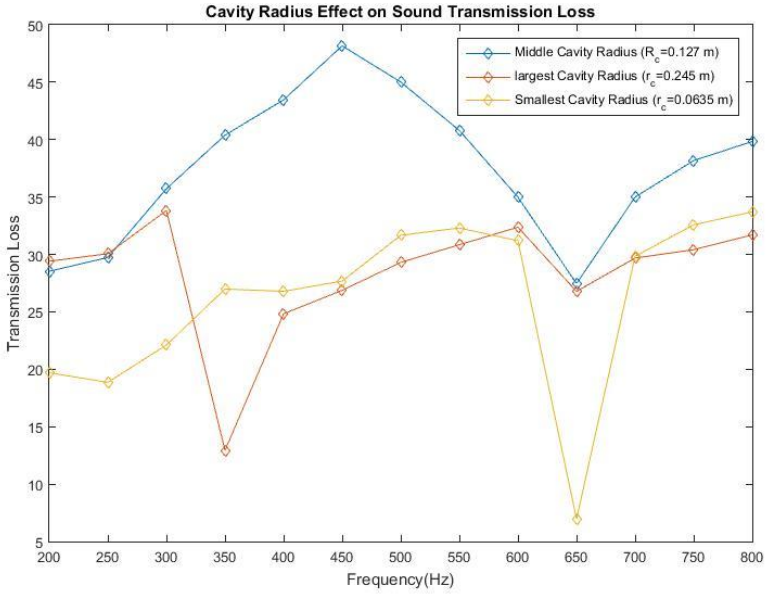

Figure 21: Cavity Radius Effect on Transmission Loss

3.1.9 The Effect of Cavity Length on Sound Transmission Loss

Another important parameter is the cavity length which also appears in cavity volume expression: $V = \pi(r_v^2) * l$, and affects both the equations (8) and (16). Three cavity lengths were used for the parametric study and the results are displayed in figures 22-25:

Main Model Geometry		Model 8 Geometry		Model 9 Geometry	
Variable	Value	Variable	Value	Variable	Value
r_n	0.0127	r_n	0.0127	r_n	0.0127
L'	0.0248	L'	0.0248	L'	0.0248
r_c	0.127	r_c	0.127	r_c	0.127
l	0.006	l	0.012	l	0.003
f_r	449.14	f_r	317.59	f_r	635.18

Figure 22: Cavity Length Comparison Models Geometries

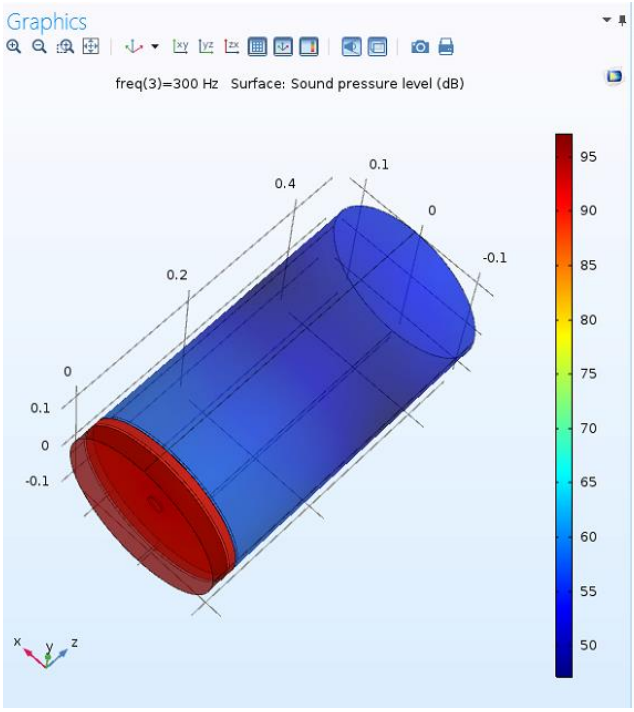

Figure 23: Doubled Cavity Length Model SPL

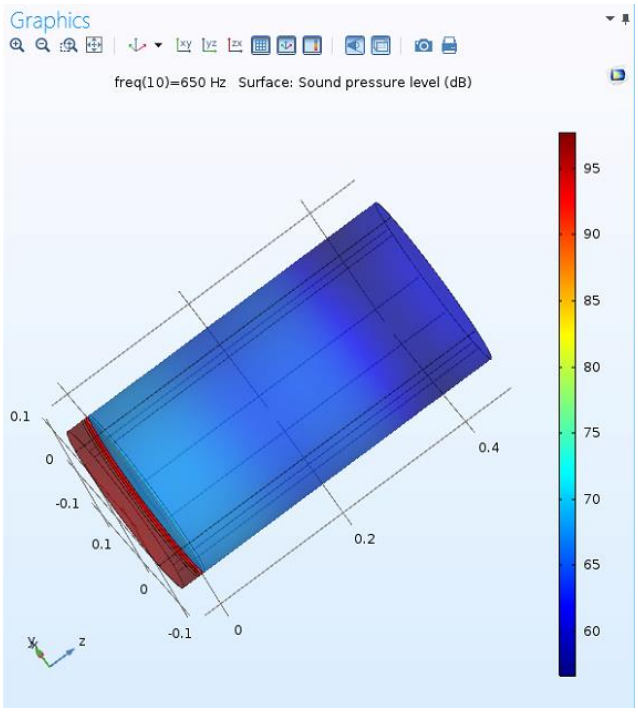

Figure 24: Reduced Cavity Length Model SPL

Also, the effect of cavity length can be summarized in the following graph:

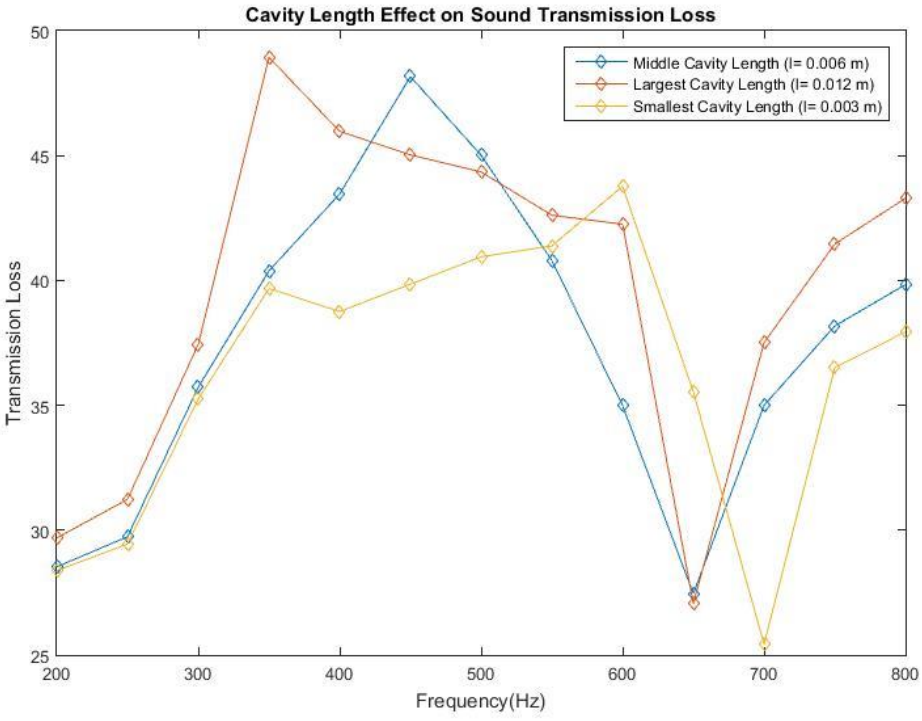

Figure 25: Cavity Length Effect on Transmission Loss

3.1.10 The Effect of Series Helmholtz Resonators on Sound Transmission Loss

Based on the discussions in the previous chapter, one of the methods to enhance the sound insulation performance of HRs is to use them in network configuration. These networks can be either parallel or series configuration or combination of both. In this section, the series configuration of Helmholtz resonators is simulated and the effect of the number of HRs used in the configuration is examined by means of modeling networks with 3-9-15 and 25 HRs and comparing the results of the simulation. For fair comparison with the nominal model, all of the HRs in the model have the same properties as the nominal model. The simulation results and the comparison plot are shown in the following figures 26-34:

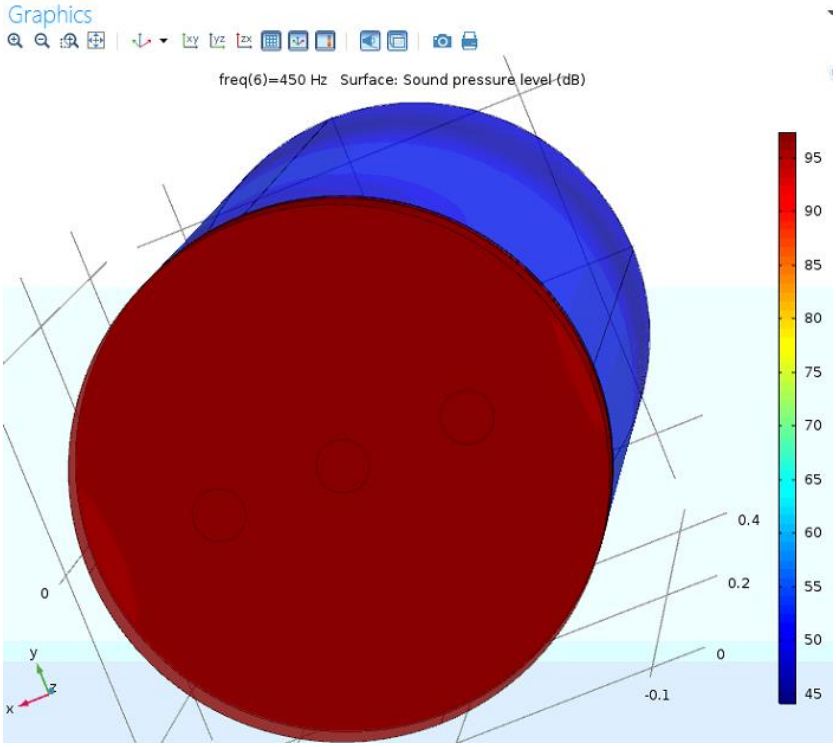

Figure 26: Front view of network of 3 HRs

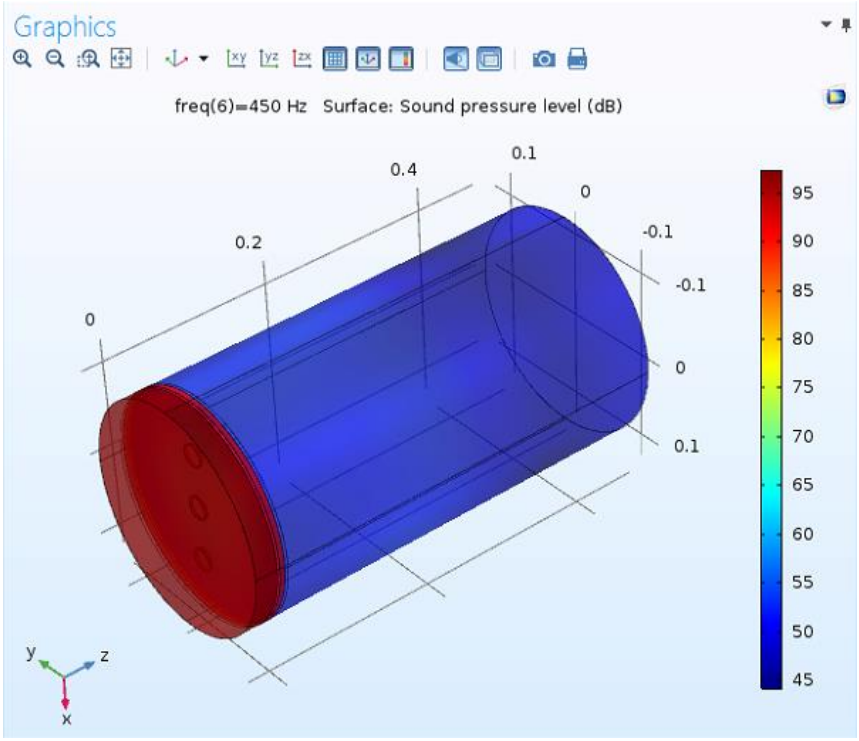

Figure 27: SPL of the Network of three HRs

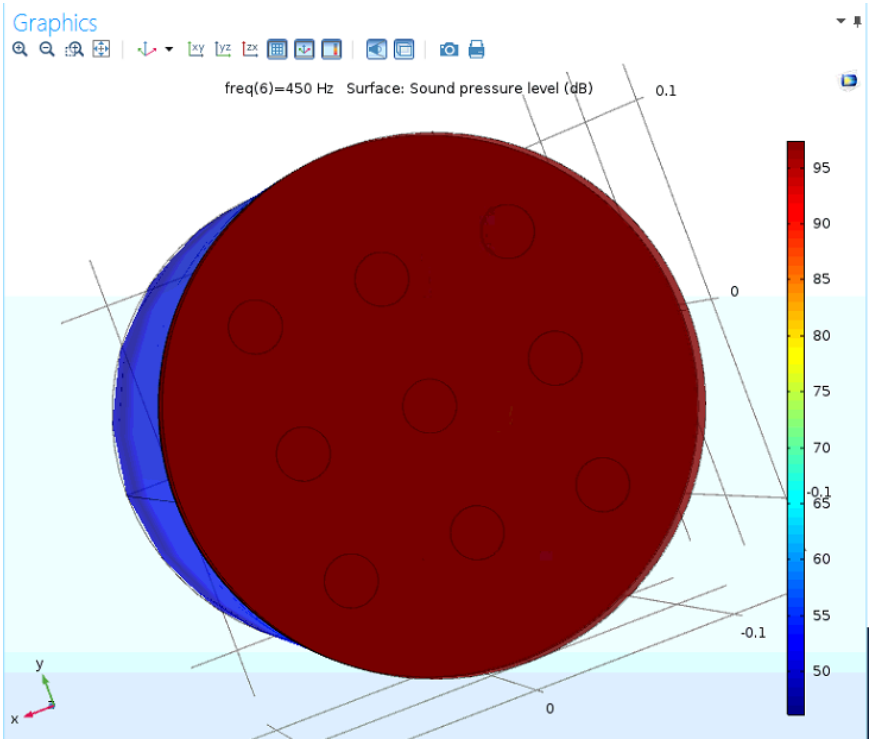

Figure 28: Front view of network of nine HRs

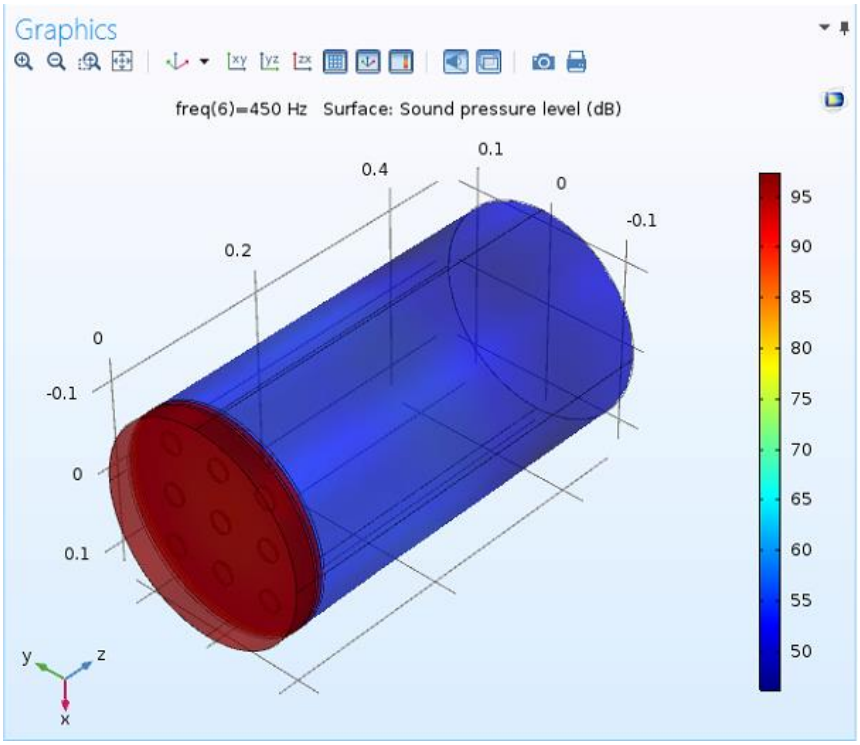

Figure 29: SPL of the Network of nine HRs

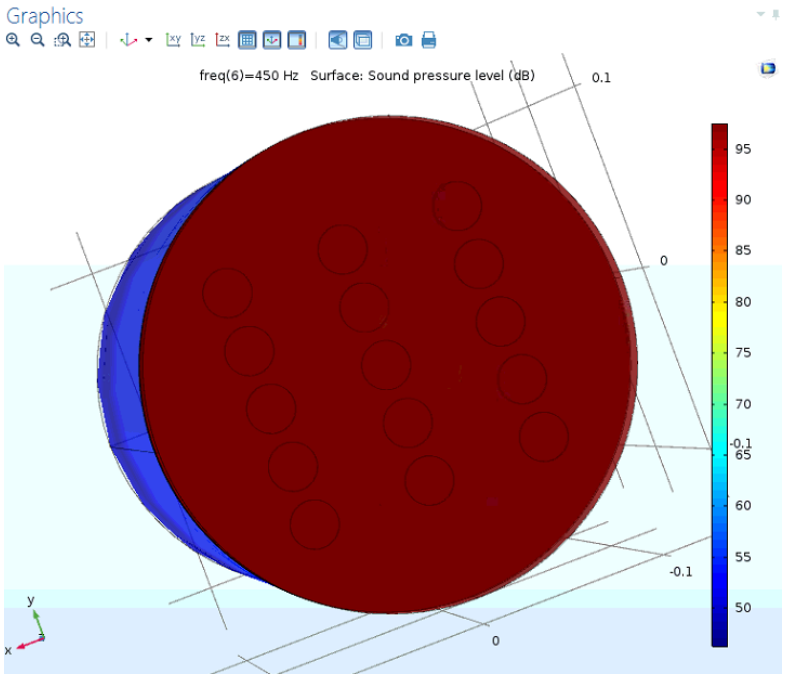

Figure 30: Front view of network of fifteen HRs

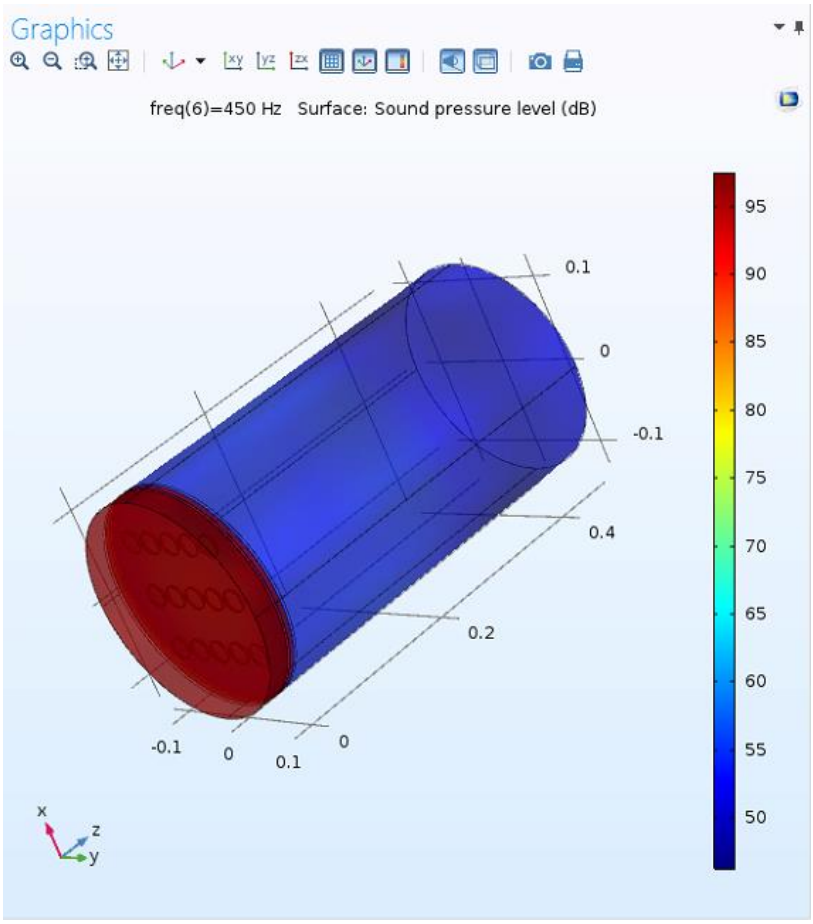

Figure 31: SPL of the Network of fifteen HRs

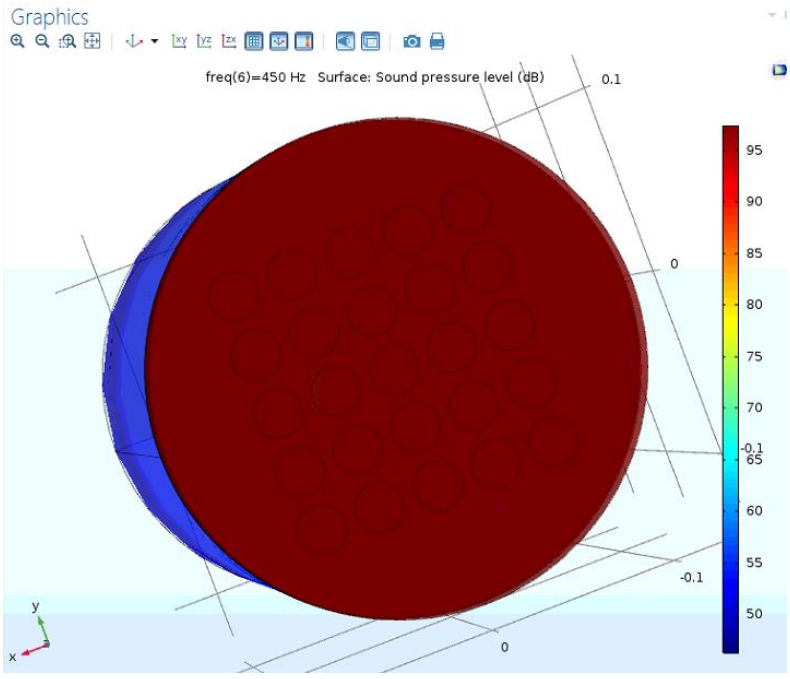

Figure 32: Front view of the network of Twenty five HRs

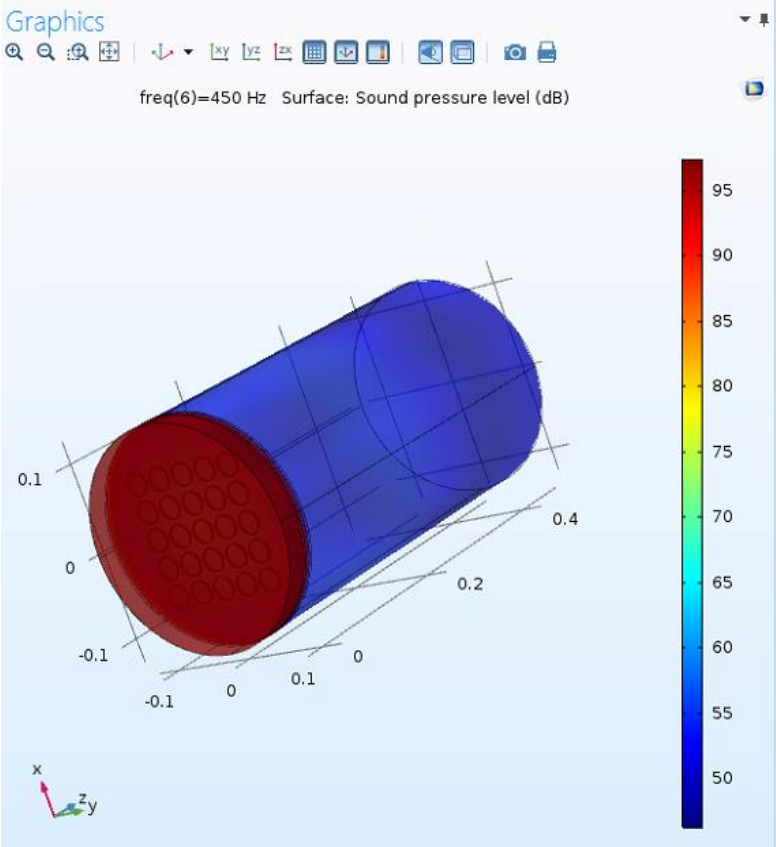

Figure 33: SPL of the Network of twenty five HRs

The effect of the number of HRs on sound transmission loss is depicted in the following graph:

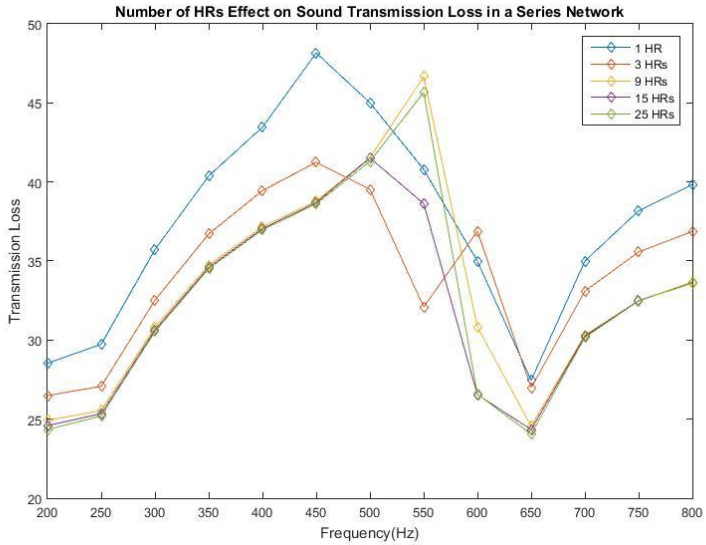

Figure 34:Number of Resonators Effect on Transmission Loss

3.1.11 The Effect of Parallel Helmholtz Resonators on Sound Transmission Loss

Another possible configuration of HRs in the network is to arrange them in a parallel configuration. In this section, the effect of using multiple HRs in a parallel configuration is studies along with the effect of the number of HRs used in the network. The simulation study used a parallel combination of 2 and 4 HRs. The simulations and the corresponding comparison plot are attached in figures 35-37:

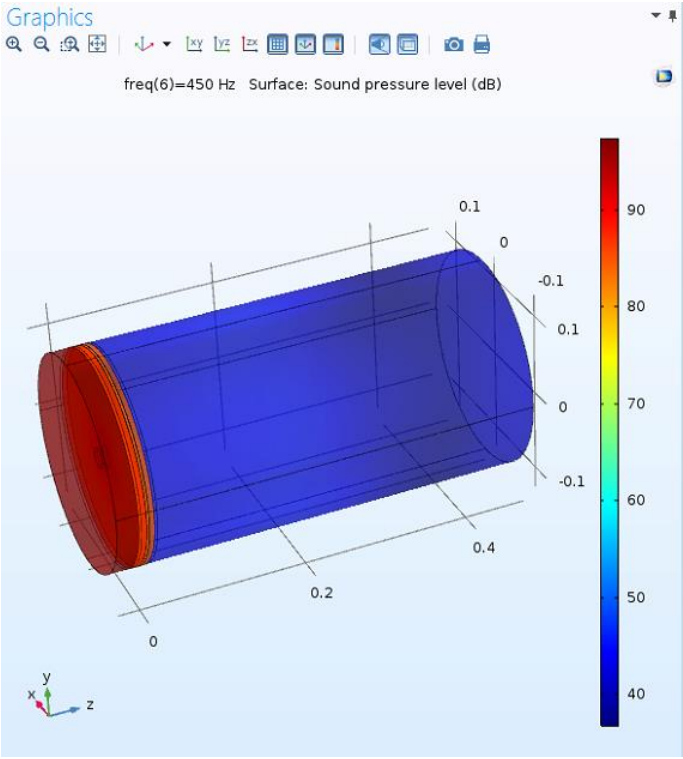

Figure 35: Parallel 2 HR Network Simulation

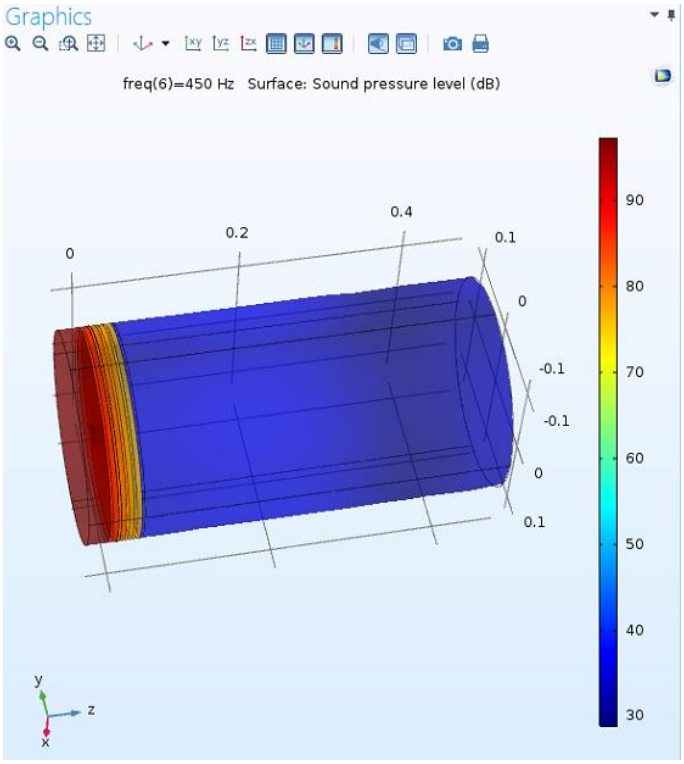

Figure 36: Parallel 4 HR Network Simulation

Based on the data from the simulation, the significance of number of parallel HRs can be summarized in the following plot:

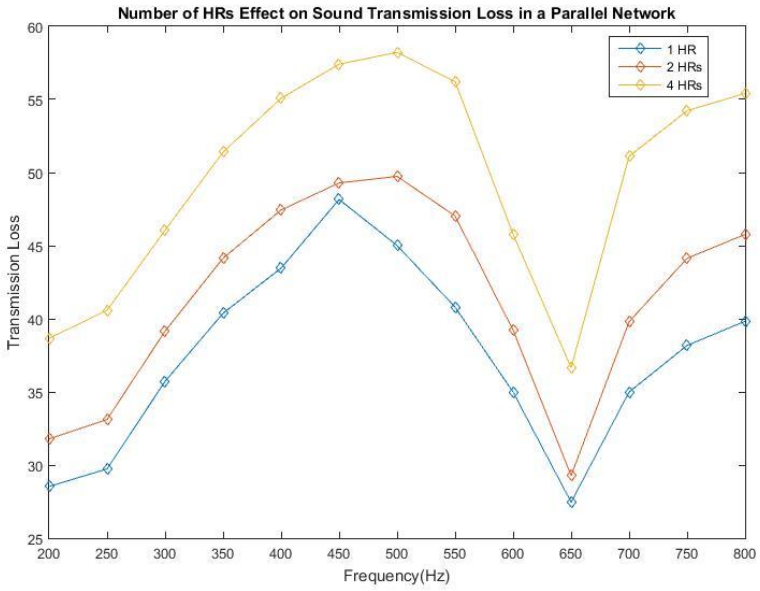

Figure 37: Number of HRs in a Parallel Network Effect on Transmission Loss

3.2 Acoustics- Porous Structure Interaction

As discussed previously, a widely used method to come up with a better sound insulation is using porous materials in the design. When a porous material exists in a design, both thermal conduction and viscous friction losses become significant. The finite element study of effect of these materials on sound propagation is accomplished using COMSOL for the Poroacoustics material model. In order to capture the effects of elastic wave dynamics in the porous matrix the Poroelastic waves module in COMSOL 5.2a was used.

3.2.1 Model Definition

For the purposes of the fair comparison the base model used in this study is the same as the nominal model that was studied in Acoustic-Structure Interaction section of the thesis except with adition of porous material. Addition of porous material changed the effective neck length for this study. The summary of the important parameters in the design of the model is shown in figure 38:

Model 10 Geometry	
Variable	Value
r_n	0.0127
L'	0.0248
r_c	0.127
l	0.012
Porous Material Length	0.003

Figure 38: Important Variables of the Main Model Lined with Porous Absorber

The porous material which is used here is a glass wool which is the default featured porous material featured in COMSOL. The primary objective of this study was to analyze the effect of porous materials on sound absorption and not the effect of specific porous material properties on sound pressure level and transmission loss. The properties of the porous material used in the study are shown in figure 39:

Glasswool Material Properties		
Parameter	Value	Unit
Tortuosity	1.06	1
Drained Density	130	kg/m3
Flow Resistivity	40000	Ns/m4
Porosity	0.094	1
Drained Shear Modulus	2200	kPa
Structural Loss Factor	0.1	1
Drained Poisson's Ratio	0	1
Viscous characteristic length	56	µm
Thermal characteristic length	110	µm

Figure 39: Glasswool Properties

3.2.2 Domain Equations

To solve for the sound pressure level of the model, COMSOL uses the Biot-Allard Model proposed in ref [41] which solves the three-dimensional poroelasticity problem in acoustics. It uses Lagrangian approach combined with an analogy to solid approach to derive a displacement finite element model. This results in large amount of calculations for large models. Therefore, an algorithm was proposed based on low frequency approximation together with frequency-dependent dissipation mechanism. COMSOL uses robust procedure to solve for sound pressure level involving porous material.

3.2.3 Boundary Conditions

The boundary conditions for Pressure Acoustics and Solid Mechanics physics the same as the previous study. In Poroelastic Waves module, two different boundary conditions are used. The first one is free boundary condition which gives the pores of the material the ability to deform under sound pressure. Also, the fixed boundary condition is applied to the back of the porous material because of the fact that the absorber is fixed in the experimental sound insulation model setup.

3.2.4 Model Simulation and Analysis

In accordance with the previous section, the three-dimensional model geometry was modeled in COMSOL. Acrylic plastic, air and the porous materials were assigned to their

corresponding domains in the material selection section. The necessary compatible boundary conditions were applied in Pressure Acoustics, Solid Mechanics and Poroelastic Waves physics modules. The multiphysics which interconnects these three modules together uses both Biot-Allard Model to couple the porous material module with the acoustics one, and force pressure conversion to couple acoustics and solid domains. The mesh properties are also the same as the previous study. The frequency range used for this study was from 200Hz to 800Hz with the increment of 50Hz. The problem was solved for the sound pressure level, stress and displacement field. The model geometry, the sound pressure level, stress and the displacement field of the model are depicted in figures 40-43:

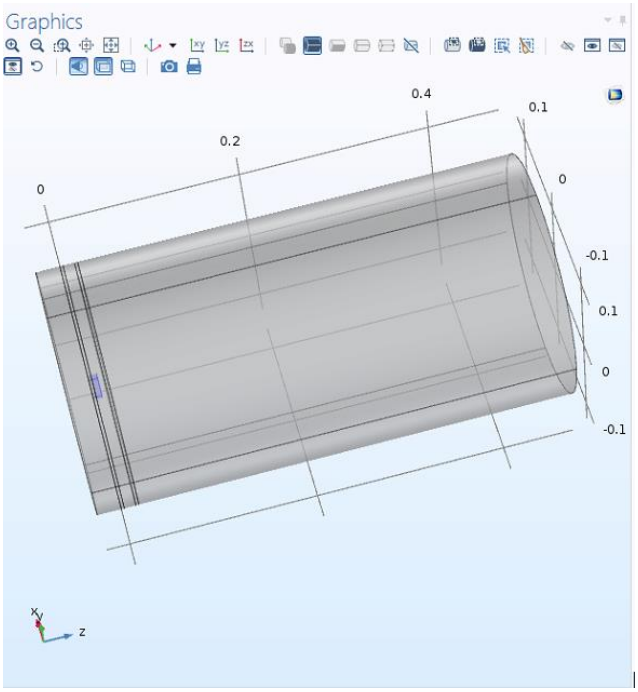

Figure 40: Model Geometry of the HR Lined with Porous Material

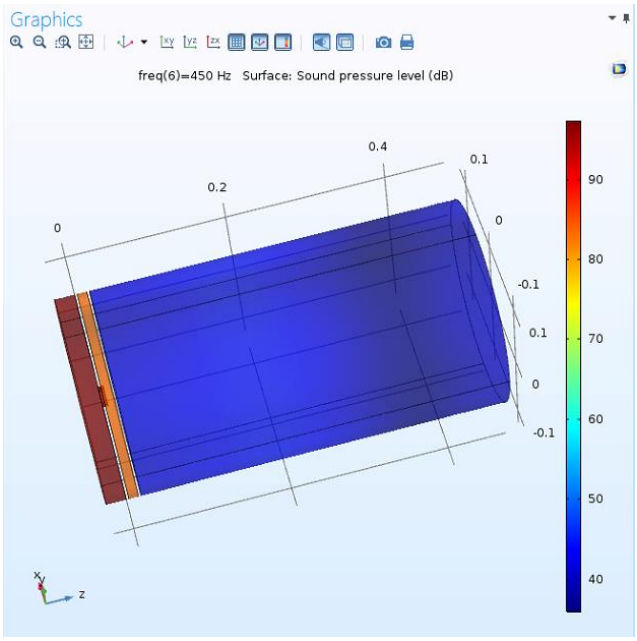

Figure 41: SPL of the HR Lined with Porous Material

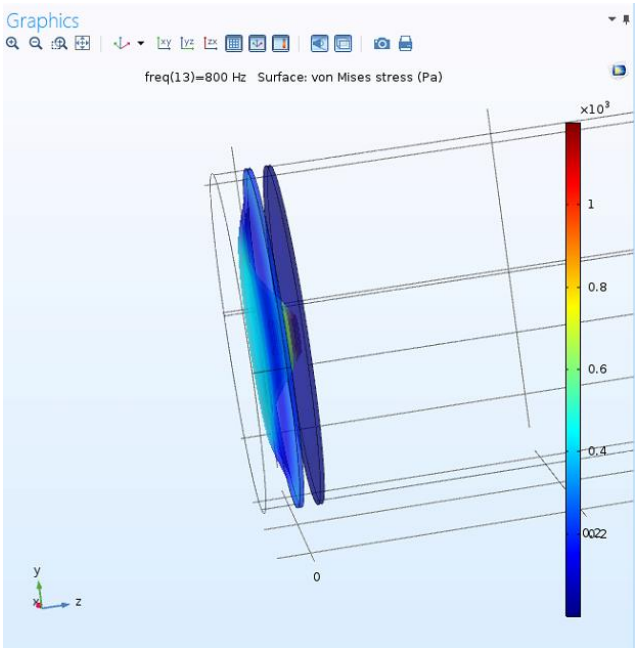

Figure 42: Stress Plot of the HR Lined with Porous Material

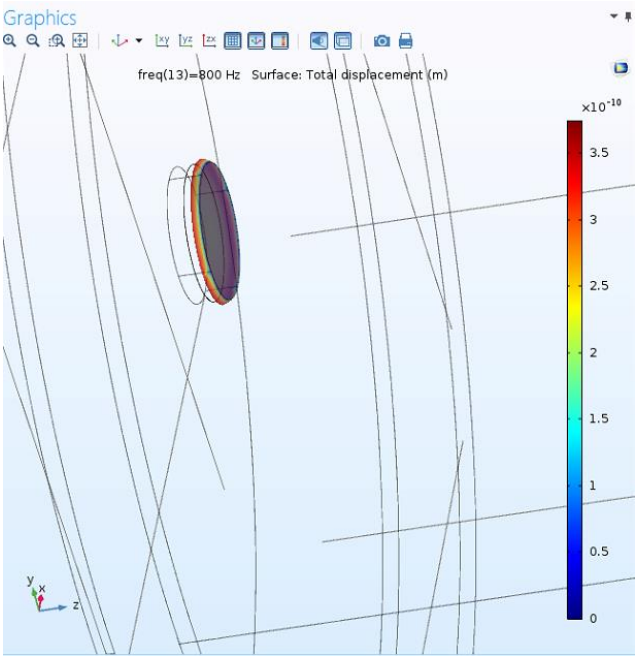

Figure 43: Displacement of the Porous Material

3.2.5 The Effect of Porous Material Thickness on Sound Transmission Loss

This section presents the study of the effect of the following parameters of the porous material: the thickness, the size and the placement of the porous material.

The purpose of the present section of this study is to examine the effect of adding a small amount of porous material right behind the neck of the HR, on sound insulation. Therefore, the size and the position of the porous material were kept the same in the simulations. The only variable that was varied for this study was the thickness of the material which is altered between 0.003, 0.006 and 0.012 millimeters. The comparison is given in the following figure:

Model 0 Geometry	
Variable	Value
r_n	0.0127
L'	0.0248
r_c	0.127
l	0.012
Porous Material Length	0

Model 10 Geometry	
Variable	Value
r_n	0.0127
L'	0.0248
r_c	0.127
l	0.012
Porous Material Length	0.003

Model 11 Geometry	
Variable	Value
r_n	0.0127
L'	0.0248
r_c	0.127
l	0.012
Porous Material Length	0.006

Model 12 Geometry	
Variable	Value
r_n	0.0127
L'	0.0248
r_c	0.127
l	0.012
Porous Material Length	0.012

Figure 44: Porous Material Thickness Comparison Model Geometries

The simulation rendered for each geometry and the sound pressure level plot are given in figures 45-47:

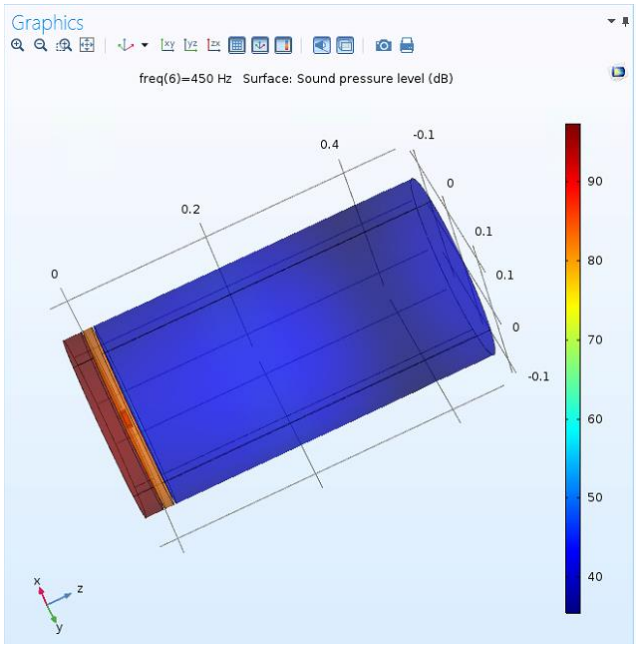

Figure 45: SPL of HR lined with 6 inch Porous Material

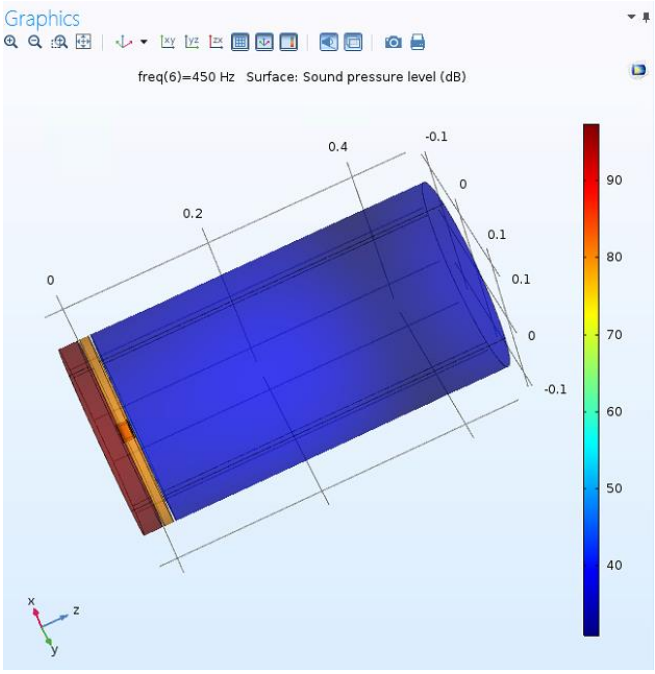

Figure 46: SPL of HR lined with 12inch Porous Material

According to the above simulations, the effect of the porous material thickness can be summarized in the following plot:

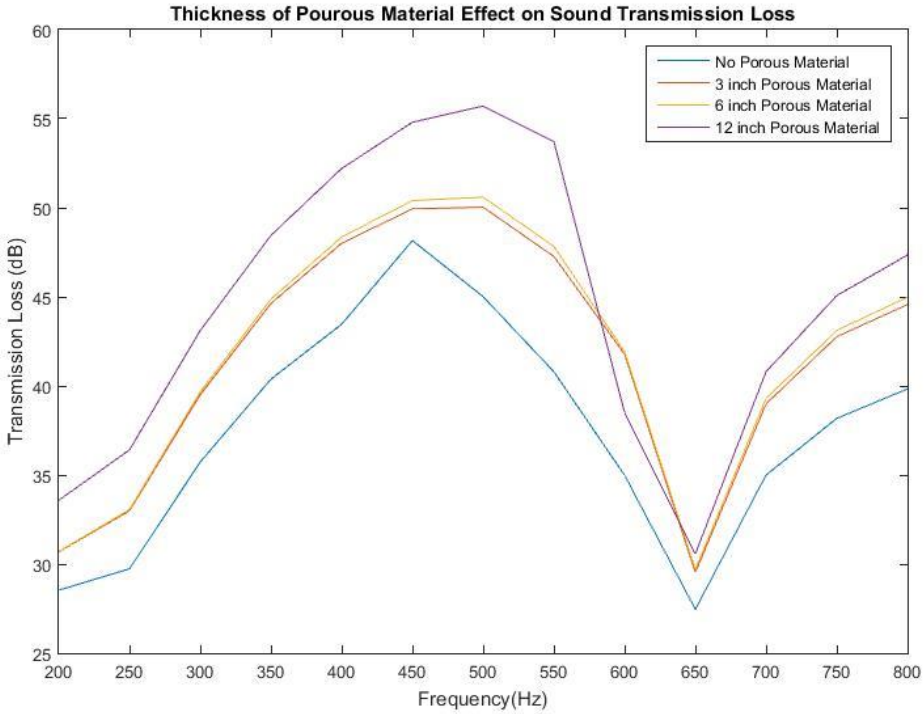

Figure 47: Porous Material Thickness Effect on Transmission Loss

CHAPTER 4: RESULTS AND DISCUSSIONS

This research study investigated various designs of HR architectures, conducted parametric study of how different HR parameters affect sound transmission properties, and also explored new concept of using combination of optimal HR configurations with the use of porous material in the design. The study included analytical treatment, simulation, and in some cases experimental validation. A comparative study of different HR configurations with and without the use of porous material was conducted and the results were reported. This chapter presents discussions of the results and provides concluding remarks. The software and the developed numerical methods are both verified, the results corresponding to each design parameter are discussed, and the best design is introduced. At the end, possible directions for future work are also presented.

4.1 Verification

In this section, both the MATLAB code corresponding to the analytical solution for side branch HRs and the numerical simulation and results are verified. The section presents results obtained from analytical modeling using MATLAB code and then these results are verified by modeling the same system using multiphysics commercial software, COMSOL.

4.1.1 Software Validation

Based on the discussions in Chapter 2, a MATLAB code was generated to analytically calculate the resonant frequencies and transmission loss of side-branch HRs. The software uses the geometry variables, a range for cavity length, and the frequencies of interest as input and solves for the resonant frequencies and the transmission losses for every geometry based on the different cavity lengths. The results from this study are validated by the results from ref [35]in which, $\frac{l}{d} = 0.01$ and$v = 4.5 * 10^{-3} m = \pi \frac{d^2}{4} * 0.01\ d \rightarrow d = 0.831\ m \rightarrow l = 8.31 * 10^{-3} m.$ As shown in the following figure, the two plots for $\frac{l}{d} = 0.01$, match perfectly.

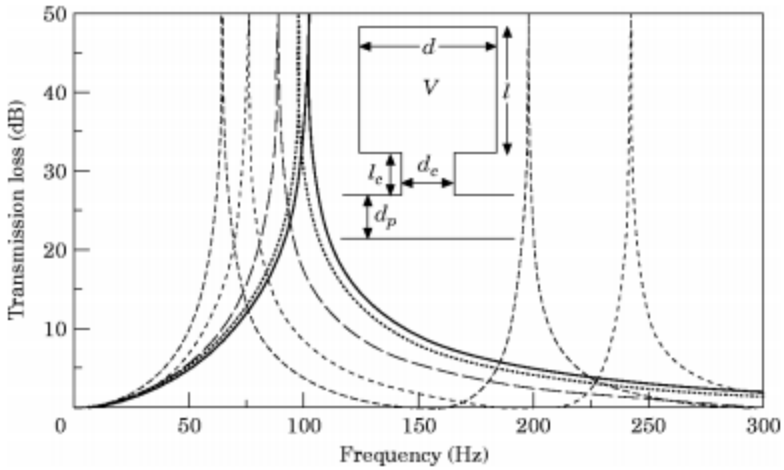

Figure 1. Theoretical Helmholtz resonator transmission loss, including wave motion in the volume (equation (4)) for a number of l/d; $V = 4500$ cm³, $d_p = 4{\cdot}859$ cm, $l_c = 8{\cdot}5$ cm and $d_c = 4{\cdot}044$ cm. ——, $l/d = 0{\cdot}01$; · · · ·, $l/d = 2{\cdot}0$; – – –, $l/d = 5{\cdot}0$; - - - -, $l/d = 10{\cdot}0$; ----, $l/d = 15{\cdot}0$.

Figure 48: Reference Paper Result Plot for Validation

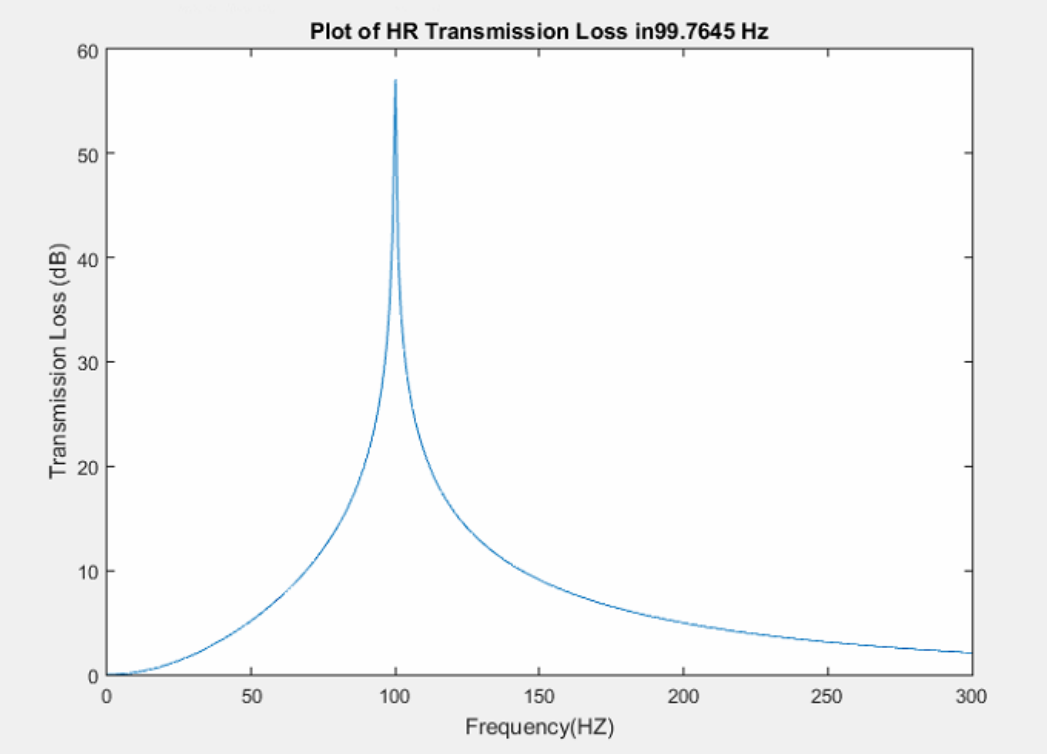

Figure 49: Plot of the results Generated by the Software for Validation

4.1.2 Numerical Analysis Validation

Although the model for which the transmission loss equation was derived (side-branch Helmholtz Resonator) is different from the model used in the study (normal incident Helmholtz Resonator configuration), COMSOL was used in conjunction with MATLAB code to verify the numerical analysis. Therefore, the side branch HR for which the verified analytical software is derived was modeled in COMSOL and the sound transmission loss is calculated based on the results form the numerical study.

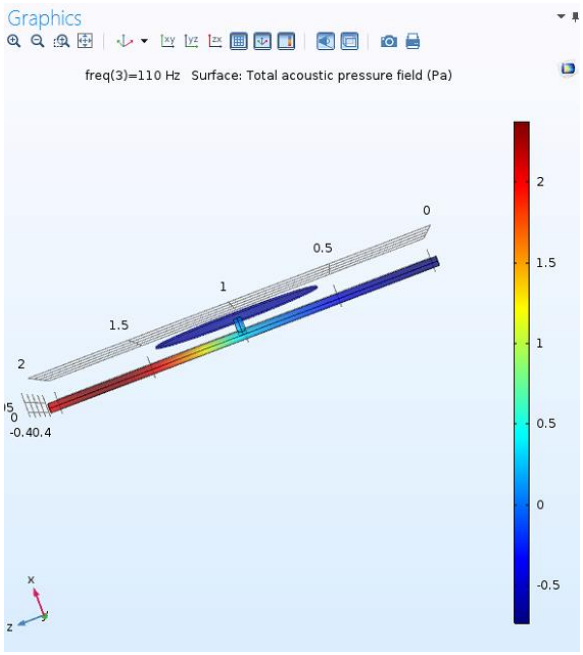

Figure 50: Acoustic Pressure Level of a Side-Branch Helmholtz Resonator

The Sound pressure level is calculated and compared to the analytical results, and the resulting plot is given in figure 51:

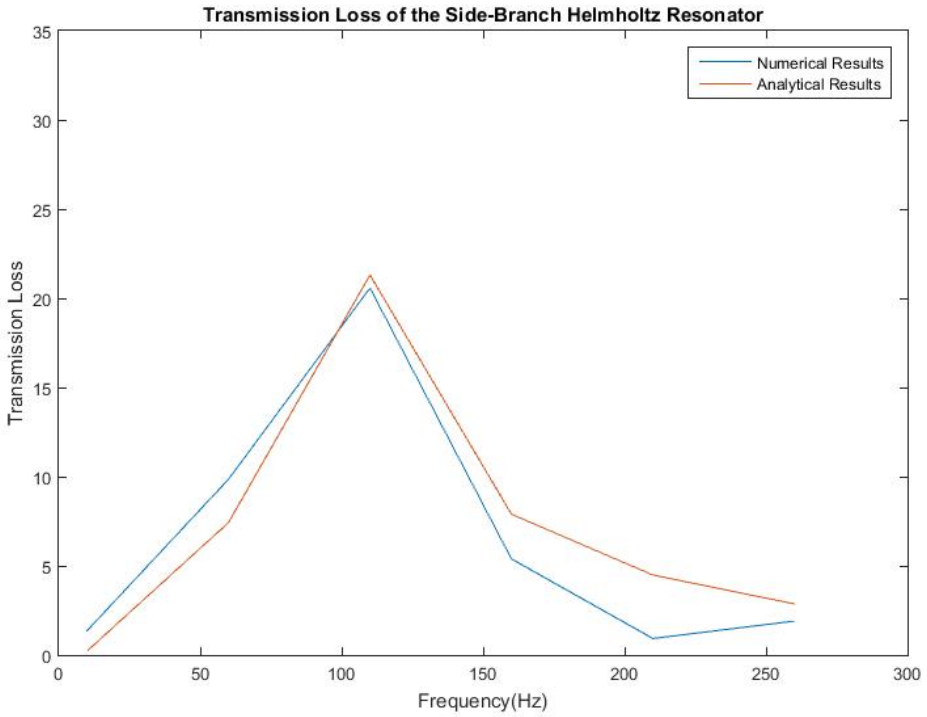

Figure 51: Transmission Loss of a Side-Branch Helmholtz Resonators

Based on figure 51, the two results overlap to a large extend and the maximum deviation is approximately 3%. This deviation is negligible considering that the numerical model includes the effect of reflection in transmission loss, whereas the analytical model does not. Also, as the analytical model reduces the multi-dimensional complexity to the simpler lumped model configuration, and neglects the viscous effects, the simplification will produce lots of deviation from the real-world problem.

4.2 Discussion

Based on the results, the three major outcomes of this study are:

- Systematic evaluation of using Helmholtz-Resonators with normal incident configuration
- Parametric study of how sound transmission loss is affected by different parameters of Helmholtz Resonators
- Evaluation of the effect of acoustic-structure interaction in sound transmission loss of Helmholtz Resonators.

- Obtained insights into what is needed in the future experimental study.

The following section discusses in greater details the effect of different design parameters of Helmholtz Resonators and the effect of acoustic-structure coupling dynamics on sound transmission performance.

4.2.1 The Impact of Distinctive Design Parameters on Sound Transmission Loss

As discussed in the previous chapters, there are several factors which affect sound transmission loss. Among them the effects of neck radius, neck length, cavity radius, cavity length, lining of porous materials, and configuring HRs in series and parallel arrangementswere analyzed.

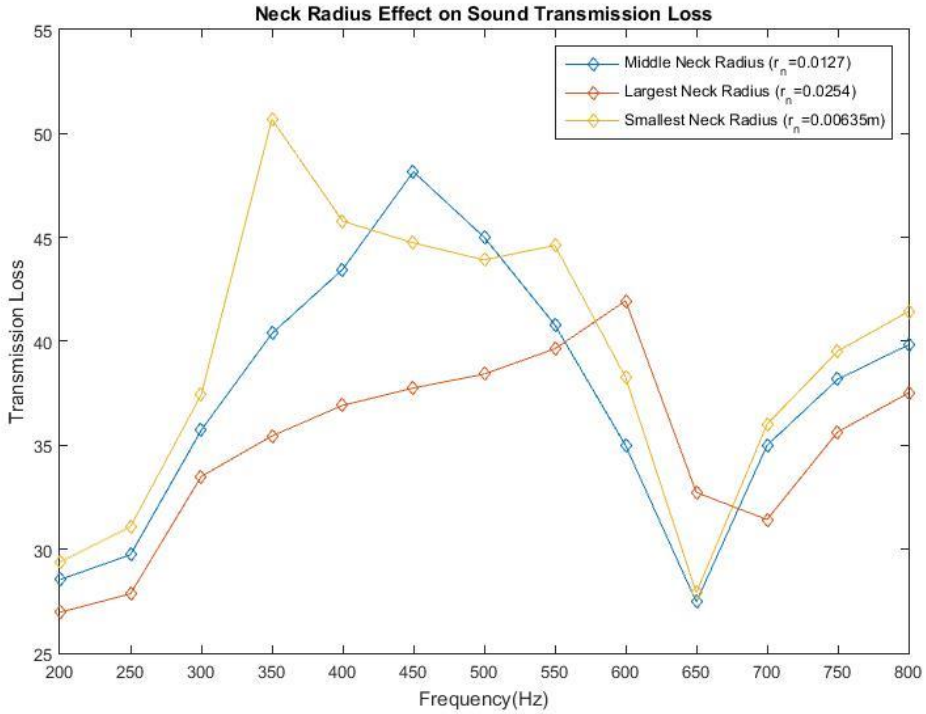

Figure 52: Neck Radius Effect on Sound Transmission Loss

As shown in figure 52, the overall performance of the HR with the smallest neck radius is better than all the other HRs except for the frequencies around the resonant frequencies of the other two models. Also, the dip frequency of 650 Hz which is the typical of resonator systems [37] is caused by the tailpipe termination and is observable in the above figure. Based on the results,

other than at the resonant frequencies of each model, doubling the neck radius resulted in an average of 3dB increase in the transmission loss.

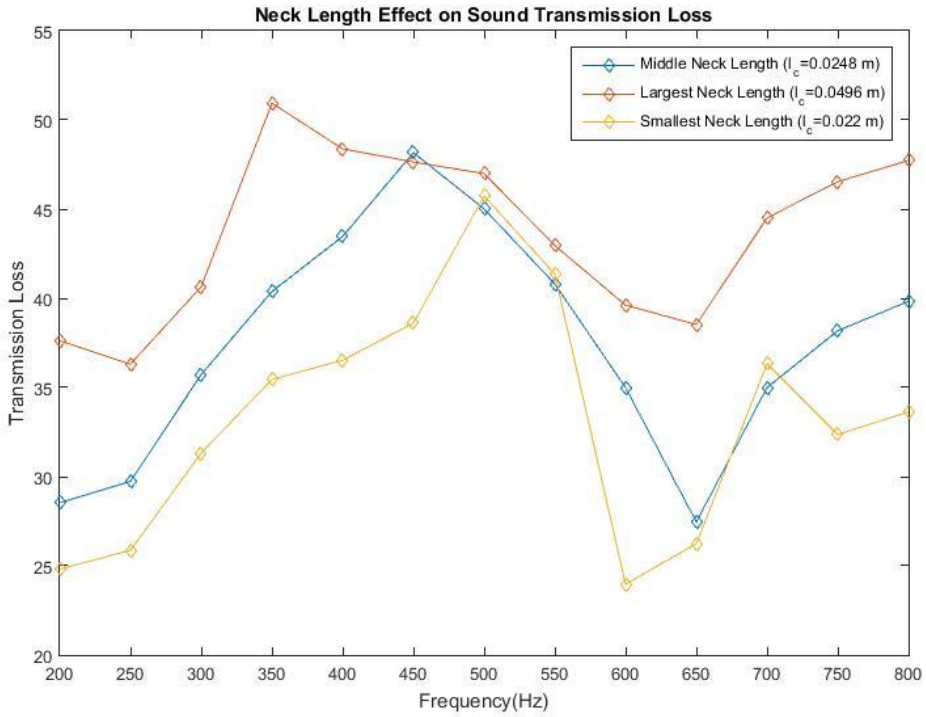

Figure 53: Neck Length Effect on Sound Transmission Loss

The effect of neck length, as depicted in figure 53, is that the transmission loss increases as the neck length increases. Also the tailpipe termination is slightly affected because it is a function of the effective length of the pipe [42]. It is evident by the plot that doubling the neck length results in an average raise of 7 dB in sound transmission loss.

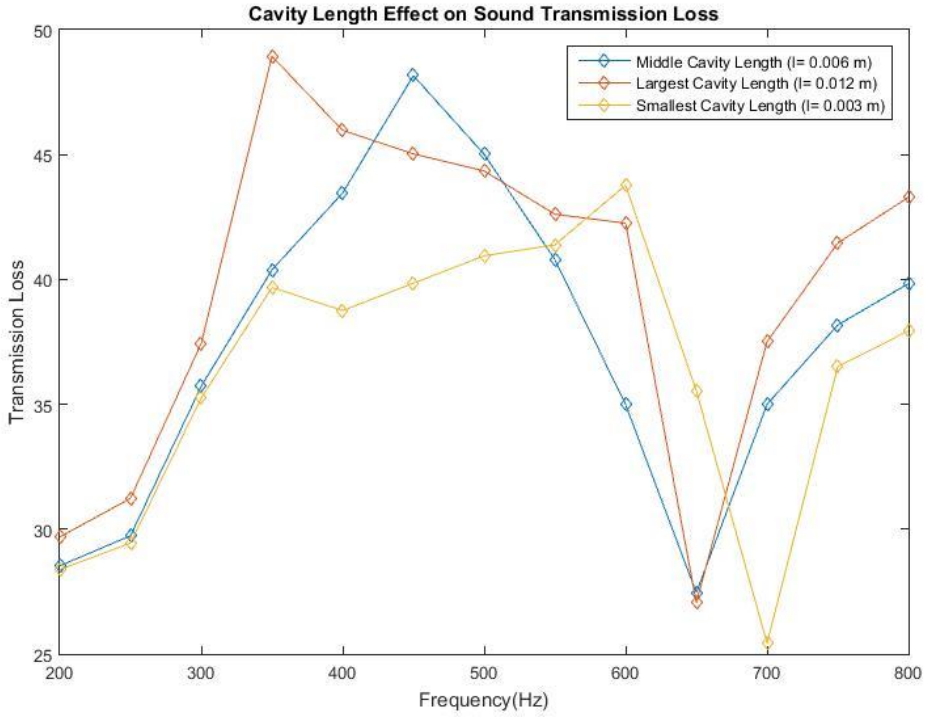

Figure 54: Cavity Length Effect on Sound Transmission Loss

The overall performance of the resonator for varying cavity length is given in figure 54. It can be observed that the bigger cavity length has better transmission loss performance except at the resonant frequencies of the ones with smaller cavity length. The tailpipe frequency is slightly affected as in the previous case as well. Also, the sound pressure is reduced as the propagation length increases which is predictable as sound pressure is expected to reduce as the sound waves propagate through a longer distance. Based on the above plot, boosting the cavity length by the factor of two results in an average increase of 3 dB in sound transmission loss.

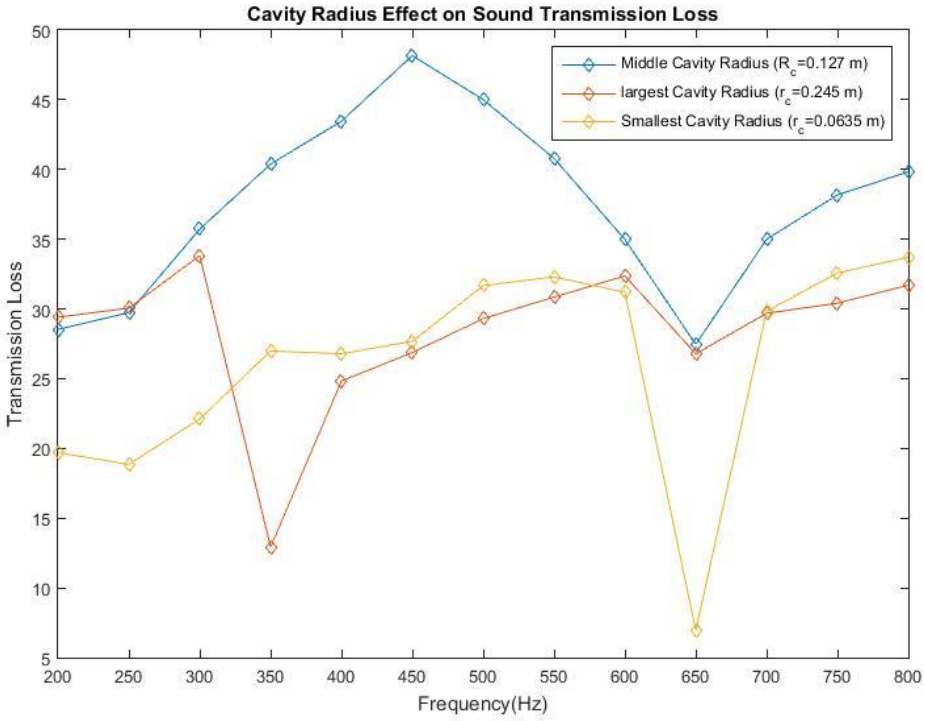

Figure 55: Cavity Radius Effect on Sound Transmission Loss

The figure 55 shows the cavity radius effect on transmission loss. It shows that the best design is the one with the mean cavity radius. As such, no definitive conclusion can be drawn in this case. As the fluid enters an expansion tank the pressure reduces to a large extent, on the other hand the less the volume of the cavity, the less the capability of the volume to transfer fluid pressure. A better analytical model is needed to examine the effect of cavity volume on transmission loss characteristics.

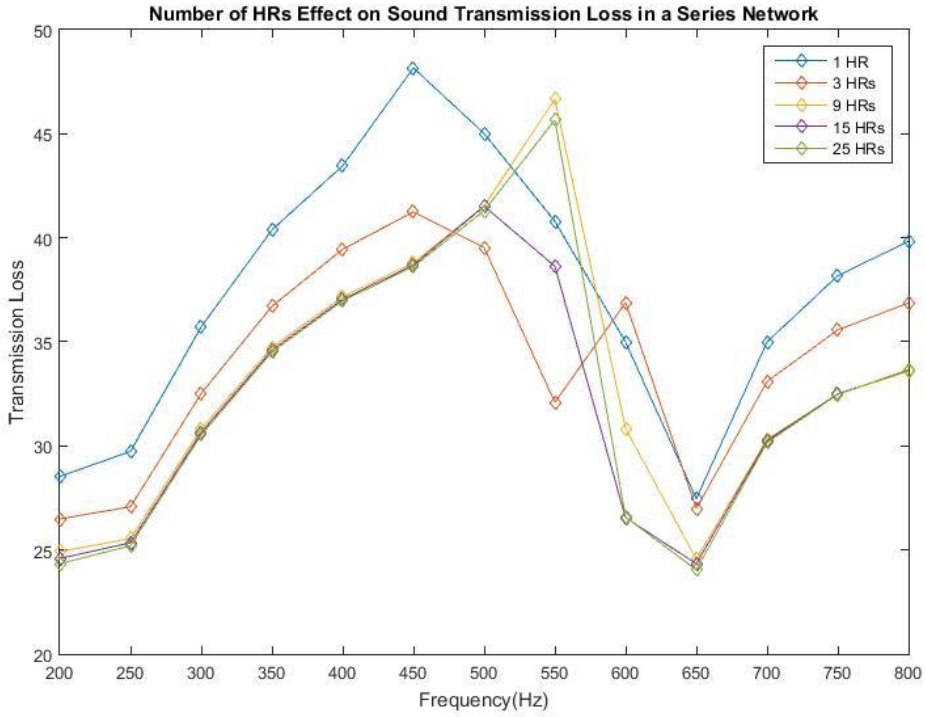

Figure 56: HR Quantity Effect on Sound Transmission Loss

The study of combining multiple HRs in series combination resulted in the plot shown in figure 56. As seen in this figure, the transmission loss is inversely proportional to the number of HRs in the series network except for the case of 9 and 25 HRs for which a noteworthy peak at the resonance frequency is observable. Based on observations from a fairly similar study in which the network of resonators were embedded between two walls [37] the resonance frequency is at or around the mean resonant frequency of the system. As in this model all the HRs have the same dimensions as the main model with the resonance frequency of 449.5. To enhance sound transmission loss using series normal incident Helmholtz resonators, it is suggested by ref [43] to partition the cavity as well.

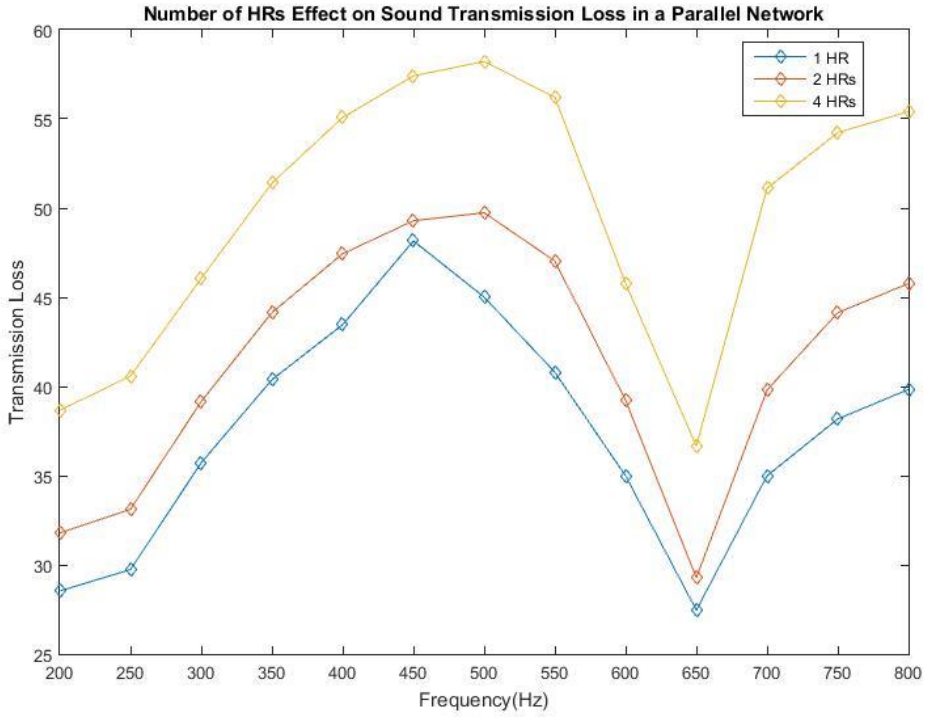

Figure 57: HR Quantity Effect on Sound Transmission Loss

The study of configuring different number of resonators in parallel configuration resulted in figure 57. As seen in this figure, as the number of parallel HRs increase, the sound transmission loss increases. The HR network having the same resonance frequency as the mean resonance frequency of the component is observable in the plot as well. Based on the data from the simulation, the average increase in sound transmission loss achieved by doubling the number of HRs in parallel network was 8.22 dB.

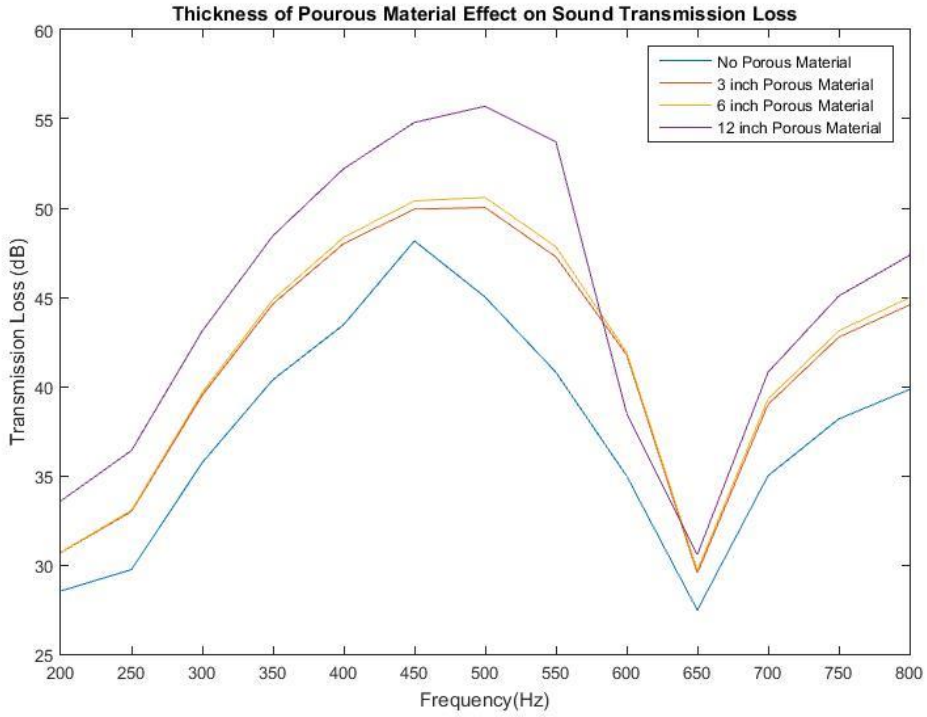

Figure 58: Thickness of Porous Material Effect on Transmission Loss

The study of porous material effect involved use of glasswool with different thicknesses and was modeled using three different COMSOL multiphysics modules (Poroelastic Waves, Solid Mechanics and Pressure Acoustics). It can be seen in figure 58 that not only adding a porous material brings about better sound insulation, but also the sound insulation performance enhances with the thickness of the material. According to the results from the simulations, doubling the porous material thickness resulted in an increase of 3.26 dB in sound transmission loss.

In summary, based on the parametric studies conducted in this work, the best design would be the one with HRs having smaller neck radius, larger neck length, and larger cavity length. Also, parallel network of HRs tends to be more promising in terms of sound insulation than the series network. Addition of a thicker porous material behind the HR neck enhances the sound insulation property as well.

4.2.2 The Effect of Structural-Acoustic Coupling on Transmission Loss

The study clearly showed that dynamics of structure-acoustic coupling plays an important role in transmission loss performance assessment and cannot be neglected. The Acoustic-Structure module in COMSOL was used in this study to evaluate this coupling effect. For comparison, the base geometry was modeled with and without coupling effects using Acoustic-Struscture Interaction module and just pure Pressure Acoustics module without structural dynamics. All the dimensions and input pressures were same. The resultant sound pressure loss performance is presented in figure 59:

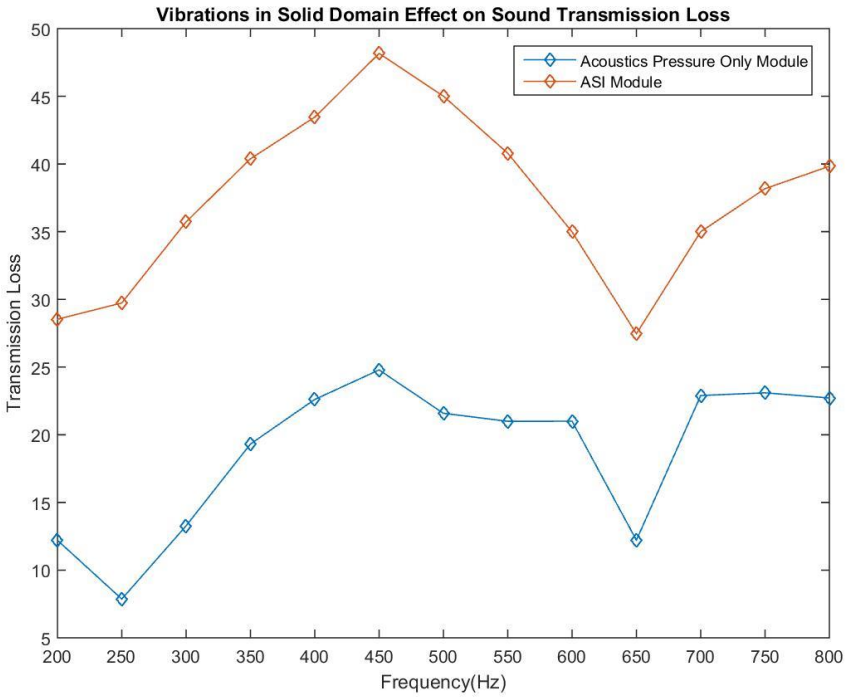

Figure 59: Solid Domain Vibrations Effect on Transmission Loss

As seen in this figure, the effect of structure-acoustic coupling on the transmission loss performance is very significant. In this particular study it was observed that the structural-acoustic coupling dynamics enhanced the transmission loss by the average of 18 dB.

4.3 Future Work

The future work in this area should address, in-depth analytical modeling of circular concentric Helmholtz Resonators with normal incident configuration. Specifically, analytical

expressions for sensitivities of different parameters of HR will be very useful in the design of such resonators in high performance sound insulation systems. Also, the effect of combining them in networks or lining them with porous materials needs to be studied analytically. Additionally, a study needs to be conducted as to which porous material will be optimal for use in lining of the HRs. An experimental study is being currently conducted at Iowa State University to validate the findings of the work presented in this thesis. The next section presents the experimental set-up that will be used to conduct thorough investigation to validate the analytical and simulation results obtained in this study. Experimental Setup:

Using ASTM standards for testing, the necessary instruments needed for the experimental setup are impedance tube, two microphones (4 microphones for more exact results), and a digital frequency analysis system. The standards also put some limitations on the dimensions and target frequencies which are computed for this study and are used in the simulations. The first variable which is effective in the data acquisition and modeling process is the diameter of the tube which determines the upper bound to the target frequency. For our study, the diameter of the tube is 5 inches (0.127 m) for which the corresponding target frequency is:

$$\mathrm{f} < 0.586\,\frac{c}{d} = 0.586 * \frac{344}{0.127} \rightarrow \mathrm{f} < 1586\ Hz \tag{49}$$

Also, the space between the mics determine the lower bound of the target frequency. For our setup, the space between the mics is 11 inches (0.2794 m) therefore the minimum frequency will be:

$$\mathrm{x} > 0.01\,\frac{c}{f} = 0.01 * \frac{344}{f} \rightarrow \mathrm{f} > 0.01\,\frac{344}{0.2794} = 12.31\ Hz \tag{50}$$

Figure 60: Impedance Tube

The microphones diameters also put an upper limit to the target frequency. It is suggested by the standard that the microphone diaphragm diameter stays less than 20% of the wavelength corresponding to the highest frequency. As the implemented microphones in the study have 0.2 inch (0.00508 m) , it will result in the following limit for our case:

$$d_m < 0.2\,\frac{c}{f} = 0.2 * \frac{344}{0.00508} \rightarrow f < 13543 \text{ Hz} \tag{51}$$

Another limitation in the usage of the microphones is the spacing should be consistent with the following upper limit:

$$\text{x} < \frac{c}{2 * f} = \frac{344}{2 * 0.2794} \rightarrow f < 615 \tag{52}$$

Figure 61: The Used Microphone for the Experiments

Additionally, based on the schematic of the measurement setup based on the standard is shown in the following figure [43], the effective parameters which should be considered in the simulations are:

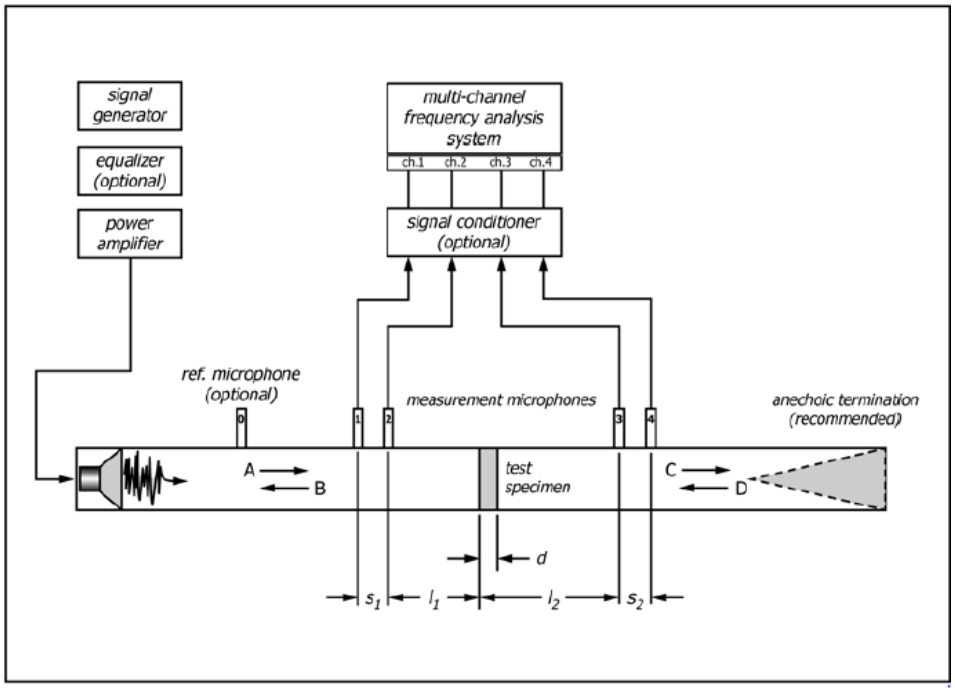

Figure 62: Schematic of the Experimental Setup[43]

Table 1: Variables Extracted based on the Experimental Standard

Variable	Value
d_c	0.127 m
f	$12.31 < f < 615$
x	0.2794
d_m	0.00508
s_1	0.1176
l_1	0.077645
d	0.01235
l_2	0.089995
s_2	0.1176

Based on the preceding explanation, these variables need to be calculated for both analytical and numerical studies. The numerical and analytical study presented in this thesis provides a good foundation for the next step of experimental work. Our future publications will present outcome of these experimental studies.

BIBLIOGRAPHY

1. Stock, C. B. Window-Related Energy Consumption in the US Residential and Commercial Building Stock. (2008).
2. Feng, L. Active feedback control of acoustic noise in 3-D enclosures. (2002).
3. Strutt, R. *Theory of Sound*. *Dover* (1945).
4. Helmholtz, H. von. *On the Sensation of Tone*. (1985).
5. Panton, R. L. & Miller, J. M. Resonant frequencies of cylindrical Helmholtz resonators. *J. Acoust. Soc. Am.* **57,** 1533–1535 (1975).
6. Chen, K. T., Chen, Y. H., Lin, K. Y. & Weng, C. C. The improvement on the transmission loss of a duct by adding Helmholtz resonators. *Appl. Acoust.* **54,** 71–82 (1998).
7. Bao C., Pan, J. Experimental study of different approaches for active control of sound transmission through double walls. *J. Acoust. Soc. Am.* **103,** 1916 (1998).
8. Claes, S. Active Control of Sound Transmission through a double wall structure. **180,** 609–625 (2014).
9. Jakob, A. & Möser, M. Active control of double-glazed windowsPart I: Feedforward control. *Appl. Acoust.* **64,** 163–182 (2003).
10. Estève, S. J. & Johnson, M. E. Reduction of sound transmission into a circular cylindrical shell using distributed vibration absorbers and Helmholtz resonators. *J. Acoust. Soc. Am.* **112,** 2840–2848 (2002).
11. Griffin, S., Lane, S. a. & Huybrechts, S. Coupled Helmholtz Resonators for Acoustic Attenuation. *J. Vib. Acoust.* **123,** 11 (2001).
12. Fahy, F. J. & Schofield, C. A note on the interaction between a Helmholtz resonator and an acoustic mode of an enclosure. *Top. Catal.* **72,** 365–378 (1980).
13. Nagaya, K., Hano, Y. & Suda, A. Silencer consisting of two-stage Helmholtz resonator with auto-tuning control. *J. Acoust. Soc. Am.* **110,** 289 (2001).

14. Mao, Q. & Pietrzko, S. Experimental study for control of sound transmission through double glazed window using optimally tuned Helmholtz resonators. *Appl. Acoust.* **71,** 32–38 (2010).

15. Xu, M. B., Selamet, A. & Kim, H. Dual Helmholtz resonator. *Appl. Acoust.* **71,** 822–829 (2010).

16. Kuroda, H. NII-Electronic Library Service. *Biol Pharm Bull.* (200AD). doi:10.1248/cpb.37.3229

17. Zhao, D., A'Barrow, C., Morgans, A. S. & Carrotte, J. Acoustic Damping of a Helmholtz Resonator with an Oscillating Volume. *AIAA J.* **47,** 1672–1679 (2009).

18. Dickey, N. S. & Selamet, A. Helmholtz resonators:one dimensional limit for small cavity length-to-diameter ratios. *J. Sound Vib.* **195,** 512–517 (1996).

19. DORIA, A. a Simple Method for the Analysis of Deep Cavity and Long Neck Acoustic Resonators. *J. Sound Vib.* **232,** 823–833 (2000).

20. Ingard, U. On the Theory and Design of Acoustic Resonators. *J. Acoust. Soc. Am.* **25,** 1037–1061 (1953).

21. Chanaud, R. C. Effects of Geometry on the resonance frequency of Helmholtz resonators, Part II. *J. Sound Vib.* **204,** 829–834 (1997).

22. Tang, S. K. On Helmholtz resonators with tapered necks. *J. Sound Vib.* **279,** 1085–1096 (2005).

23. Selamet, A. & Lee, I. Helmholtz resonator with extended neck. *J. Acoust. Soc. Am.* **113,** 1975–1985 (2003).

24. Yang, D., Wang, X. & Zhu, M. The impact of the neck material on the sound absorption performance of Helmholtz resonators. *J. Sound Vib.* **333,** 6843–6857 (2014).

25. Mulholland, K. A. The effect of sound-absorbing materials on the sound insulation of single panels. *Appl. Acoust.* **2,** 1–7 (1969).

26. Narang, P. P. Material parameter selection in polyester fibre insulation for sound transmission and absorption. *Appl. Acoust.* **45,** 335–358 (1995).

27. Lyons, A. *Materials for architects and builders*. (2007).

28. Jelle, B. P., Baetens, R. & Gustavsen, A. Aerogel Insulation for Building Applications. *Sol-Gel Handb.* **3–3,** 1385–1412 (2015).

29. Gibiat, V., Lefeuvre, O., Woignier, T., Pelous, J. & Phalippou, J. Acoustic properties and potential applications of silica aerogels. *J. Non. Cryst. Solids* **186,** 244–255 (1995).

30. E-1050, A. Standard Test Method for Impedance and Absorption of Acoustic Materials using a Tube two Microphones and a Digital Frequency Analysis System. *Am. Soc. Test. Mater.* 1–12 (1998). doi:10.1520/E1050-12.2

31. ASTM. Standard Test Method for Field Measurement of Sound Power Level by the Two-. *Astm* **61,** 1–7 (2015).

32. Alster, M. Improved calculation of resonant frequencies of Helmholtz resonators. *J. Sound Vib.* **24,** 63–85 (1972).

33. Kinsler, L. *Fundamentals of acoustics*. (1982).

34. Bies, D. A. & Hansen, C. *Engineering Noise Control*. (2003).

35. Selamet, A. & Dickey, N. S. Theoretical, computational and experimental investigation of Helmholtz resonators with fixed volume:lumped versus distributed analysis. *J. Sound Vib.* **187,** 0–3 (1984).

36. Selamet, A. & Radavich, P. M. Circular concentric Helmholtz resonators. *J. Acoust. Soc. Am.* **101,** 41–51 (1997).

37. Prydz, R. A., Wirt, L. S., Kuntz, H. L. & Pope, L. D. Transmission loss of a multilayer panel with internal tuned Helmholtz resonators. *J. Acoust. Soc. Am.* **87,** 1597–1602 (1990).

38. Beranek, L. L. & Work, G. A. Sound Transmission through Multiple Structures Containing Flexible Blankets. *J. Acoust. Soc. Am.* **21,** 419–428 (1949).

39. Seddeq, H. S. Factors Influencing Acoustic Performance of Sound Absorptive Materials. *Aust. J. Basic Appl. Sci.* **3,** 4610–4617 (2009).

40. COMSOL. Acoustic-Structure Interaction. 1–16

41. Atalla, N., Panneton, R. & Debergue, P. A mixed displacement-pressure formulation for poroelastic materials. *J. Acoust. Soc. Am.* **104,** 1444–1452 (1998).

42. Selamet, a., Dickey, N. S. & Novak, J. M. A Time-Domain Computational Simulation of Acoustic Silencers. *J. Vib. Acoust.* **117,** 323 (1995).

43. Liu, J. & Herrin, D. W. Enhancing micro-perforated panel attenuation by partitioning the adjoining cavity. *Appl. Acoust.* **71,** 120–127 (2010).